Assessment of carbon assimilation in a tropical forest of Western Ghats, India

Shijo Joseph
March, 2009

Course Title:	Geo-Information Science and Earth Observation for Environmental Modelling and Management
Level:	Master of Science (MSc)
Course Duration:	September 2007 - March 2009
Consortium partners:	University of Southampton (UK) Lund University (Sweden) University of Warsaw (Poland) International Institute for Geo-Information Science and Earth Observation (ITC) (The Netherlands)
GEM thesis number:	2007-07

Assessment of carbon assimilation in a tropical forest of Western Ghats, India

by

Shijo Joseph

Thesis submitted to the International Institute for Geo-information Science and Earth Observation in partial fulfilment of the requirements for the degree of Master of Science in Geo-information Science and Earth Observation for Environmental Modelling and Management

Thesis Assessment Board

Chairman: Prof. Alfred de Gier
External Examiner: Prof. Terry Dawson
Internal Examiner: Dr. Yousif Hussin
First Supervisor: Dr. Patrick van Laake
Second Supervisor: Prof. Lars Eklundh

ITC International Institute for Geo-Information Science and Earth Observation
Enschede, The Netherlands

Abstract

Terrestrial vegetation plays a significant role in climate balance and biogeochemical cycling. The feedback interactions between the biosphere and atmosphere and the identification of mechanisms which maintains these interactions is one of today's scientific priorities in view of the climate change debate. However, the methods to assess these interactions operationally are widely criticized. The present attempts to validate the algorithms are biased towards temperate and neotropical areas. In this context, the present study assesses the implementation of an alternative algorithm in an old world tropical biodiversity hotspot.

The model is formulated by taking into consideration of the local environmental conditions. The maximum light use efficiency of vegetation types (ε_0), and the controlling factors which limits ε_0, the amount of incident PAR and fraction of PAR that canopy absorbs are combined together to estimate the carbon assimilation. The result is compared with the existing operational algorithm (MODIS GPP product) and the difference is analysed in terms of structure of algorithm and resolution of input datasets.

The results indicated that the lower elevation tropical wet evergreen forest assimilates the highest amount of carbon whereas montane grasslands assimilate lowest level of carbon. Tropical deciduous forests showed an assimilation rate which was almost equal to evergreen forest during wet season. The comparison with globally derived estimate (MODIS GPP product) showed that both the estimates are significantly different. The change in magnitude of estimate was not because of algorithm difference, but it was due to the resolution of the input datasets. The estimates using global datasets of 1^0 resolution was almost three times higher than the estimates using ground measurements.

The study leads to several ecological insights and practical implications in the carbon assimilation monitoring. Daily data at 500 m resolution by MODIS is quite reasonable to understand the spatial and temporal dimensions of vegetative surfaces. Advanced vegetation index such as EVI can outperform conventional index like NDVI. Soil moisture condition could be adequately represented by MODIS shortwave infrared indices. Physical constraints can limit carbon assimilation capacity of vegetation types. GPP estimation in heterogeneous mountain areas needs high resolution temperature and IPAR datasets. Resolution of the input datasets plays a major role rather than algorithm in carbon assimilation estimation.

Dedicated to,

My Beloved Teacher – Dr. R. Satheesh

Acknowledgements

My special thanks to GEM Consortium and European Union for facilitating the study. All the national coordinators and program secretaries are kindly acknowledged.

It is my great pleasure to remember that I have a supervisor who is theoretically strong, technically superior and morally supportive. Without his constant inspiration, valuable guidance and logical organization, the work was not viable. With a profound sense of gratitude, I express my sincere thanks to Dr. Patrick van Laake for his patience and kindness in guiding and sharing his experience throughout the project period.

The feasibility of the work was first recognized by my second supervisor, Prof. Lars Eklundh, who acted as the backbone of the project from the first day of the discussion to the final day of submission. His constant encouragement, timely advices, and moreover the understanding he has shown throughout the project period was very vital for me to finish this work. I take this opportunity to say my sincere thanks to you for your direction and magnanimity.

A number of people enriched the project with constructive comments and creative insights. The comments by Prof. Terry Dawson and Prof. Petter Pilesjo during the proposal defence and Prof. Alfred de Gier and Dr. Iris van Duren during mid-term presentation are kindly acknowledged.

I am extremely thankful to Prof. A. P. Thomas, who sparkled my mind with the idea to work in the carbon sequestration of Indian forest. My dearest friends at school of Environmental Sciences, Mahatma Gandhi University especially Ajay Balakrishna, are deeply acknowledged.

Many of the datasets used in the project came from different sources. Dr. M. S. R. Murthy, Dr. V. K Srivastava and Dr. S. Sudhakar, National Remote Sensing Centre, Indian Space Research Organization permitted me to use the plot data, in addition to provide constant support. Dr. Jose Kallarackal, Kerala Forest Research Institute and Mr. Sekhar L. K, ITC provided weather data. Prof. Alan Robock, Rutgers University provided soil moisture data.

The data analysis made easy with the tips from few expert programmers. Mr. Jose Beltran Abaunza, Mr. Willem Nieuwenhuis and Dr. Ulanbek D. Turdukulov are kindly acknowledged.

Prof. Edward J. Milton, Dr. Jadu Dash and Prof. Ben Smith were kindly acknowledged for the beneficial discussions and constant support during the program. The support from my batch mates especially the Indian friends, are kindly remembered.

Finally, but most importantly, my gratitude goes to the most precious gift in my life i.e., my family. If I have achieved anything in my life, it is due to my family who supported me at all contexts with their love and prayer. I could see my land through the eyes of Anitha who have murmured thousands of things and made everyday as a new day.

List of Abbreviations

APAR	: Absorbed Photosynthetically Active Radiation
CASA	: Carnegie-Ames-Stanford Approach
DOY	: Day of the Year
EC-LUE	: Eddy Covariance Light Use Efficiency
EVI	: Enhanced Vegetation Index
FPAR	: Fraction of Photosynthetically Active Radiation
GBH	: Girth at Breast Height
GLO-PEM	: Global Production Efficiency Model
GPP	: Gross Primary Productivity
IPAR	: Incident Photosynthetically Active Radiation
LSWI	: Land Surface Water Index
LUE	: Light Use Efficiency
NDVI	: Normalised Difference Vegetation Index
P	: Phenology
S.M	: Soil Moisture
SIWSI	: Shortwave Infrared Water Stress Index
SRTM	: Shuttle Radar Topographic Mission
T	: Temperature
VPD	: Vapour Pressure Deficit
VPM	: Vegetation Production Model
W	: Water

Table of Contents

List of figures

List of tables

1. Introduction

1.1. General Research background

The earth's climate is determined by a number of complex connected physical, chemical and biological processes occurring in the atmosphere, land and ocean. The radiative properties of the atmosphere, a major controlling factor of the earth's climate, are strongly affected by the biophysical state of the earth's surface and by the atmospheric abundance of a variety of trace constituents. The relations between these two components are generally nonlinear and may produce negative or positive feedbacks to the climate system. A wide range of direct and indirect measurements confirm that the atmospheric mixing ratio of CO_2 has increased globally by about 100 ppm over the last 250 years, from a range of 275 to 285 ppm in the pre-industrial era (AD 1000–1750) to 379 ppm in 2005 (IPCC 2007). Since the beginning of continuous measurements of the atmospheric CO_2 concentration at the end of the 1950s (Keeling 1960), the average rate of increase is 1.4 ppm/yr (IPCC 2007). Some of the possible biogeophysical effects of this increase includes extinction of species especially endemics (Thomas et al. 2004, Ishigami et al. 2005, Malcolm et al. 2006), migration of boreal forest northward into tundra (Otterman et al. 1984, Brovkin et al. 2003, IPCC 2007) and shift of tropical rainforest to savannah (Dickinson and Henderson-Sellers 1988, Sukumar 1995).

Terrestrial ecosystems absorb approximately 60 Gt of carbon annually while releasing the same amount (Janzen 2004). As the estimated annual turnover between the atmosphere and terrestrial ecosystems is approximately 120 Gt, much greater than the amount of fossil fuel emissions (5 Gt), small alterations in the terrestrial carbon balance are likely to have significant impact on atmospheric CO2 concentrations (Hilker et al. 2006). Therefore, operational monitoring of biosphere and biosphere-atmosphere carbon exchange is an inevitable step to be undertaken to ensure habitability of the earth. Diagnostic models that utilize climate constrained light-use and production efficiency equations provide an effective method for achieving this goal, as demonstrated by products such as MODIS MOD17 (Running et al. 2004, Heinsch et al. 2006), CASA (Potter et al. 1993, 2003, Lobell et al. 2002), and GLO-PEM (Prince and Goward 1995, Goetz et al. 1999). These spatiotemporal estimates are subject to errors and uncertainties arising from state variables (for example, land cover, plant biomass), interpolated meteorology, model logic, and model parameters. Quantifying model errors and uncertainties allows carbon flux estimates to be reported with known levels of confidence (Heinsch et al. 2006, Zaehle et al. 2005, Kyriakidis and Dungan 2001), and identifying and minimizing these inaccuracies will improve model predictions.

In particular, NASA land products MOD17A2/A3, which provide 8-day estimates of gross primary production (GPP) and annual estimates of net primary production (NPP) (Running et al. 2004) is one of the primary sources of information on carbon exchange at the global scale. However, several recent studies have highlighted limitations of this model (Heinsch et al. 2006, Turner et al. 2005, and Yuan et al., 2007). The most serious limitation arises from the uncertainties of coarse resolution DAO (Data Assimilation Office is now replaced by the Global Modeling and Assimilation Office) meteorological reanalysis data used in MOD17 (Heinsch et al. 2006, Zhao et al. 2006). MOD17 also depends on estimates of light use efficiency (LUE) obtained from lookup tables based on vegetation type, which may contain errors either in the original estimate of LUE for a particular vegetation type or in the assignment of vegetation type to a pixel. Although it may be possible to correct problems with the MOD17 by improving the accuracy of the meteorological and other data inputs, it is also worthwhile to explore alternative methods for estimation of global GPP.

Tropical forests are huge storehouse of carbon accounting as much as 40% stored as terrestrial biomass (Dixon et al. 1994). Studies based on long term ecological plots report accumulation of carbon at a mean rate of 0.71 ± 0.34 tons C/ha/yr in mature, undisturbed neotropical forests (Phillips et al. 1998). Koerner (2004) argues that accurate assessment of trends in forest carbon balance requires long-term monitoring of many replicate plots or very large plots; lacking these studies, the net carbon balance of undisturbed tropical forests cannot be authoritatively assessed based on in situ studies. Baker et al. (2004) present an updated analysis from Philips et al. (2004) by considering several methodological issues and concluded that neotropical forests are accumulating carbon at a rate of 0.9 ± 0.32 tons C/ha/yr. If this value is extrapolated for the whole Neotropical moist forest area, the net carbon sink would be 0.6 Gt C/yr (Malhi and Phillips 2004). However, assessments of carbon sink in old world tropics (≈ 50% global moist forest is in Afro-Asian tropics) is not well represented in literature. If African and Asian tropics were to show a similar trend like in neotropics, the associated tropical net carbon sink would be about 1.2 Gt C/yr.

India has a geographical area of 328 Mha, of which 68 Mha are under forest cover (FSI 2003). India is a known mega-diversity country, contributing 7% (with 33% endemism) to the total phytodiversity existing in the world. Out of 25 biodiversity hotspots listed by Myer et al (2000), two are located in India. The forests of India are broadly classified into 14 major types (Champion and Seth, 1968). Of these, the tropical forests occupy 51 Mha or 80% of the forested area. Based on limited number of studies, it is estimated that carbon storage capacity of Indian forests are in the range of 1.9–4.1 Gt C. Mainly two types of approaches have been taken to reach such conclusion. Using phytomass carbon densities based on ecological studies and remote sensing-based forest areas, forest phytomass C pool was estimated in the range of 2.5–4.1 Gt C (Ravindranath et al. 1997). Using field inventory of growing stock volume and biomass expansion factors relating wood volume to biomass, forest phytomass C pool was estimated as 1.9–4.0 Gt C (Dadhwal and Nayak 1993, Dadhwal and Shah 1997). The estimated carbon densities per hectare of forest phytomass are mostly in the range of 50–68 tons (Chhabra and Dadhwal 2004). Except these few gross estimates carbon stock, there are no studies on carbon exchange as a sink or source at frequent time intervals reported.

India is presently a non–Annex I country in the Kyoto Protocol of the UNFCCC and is exempt from binding GHG emissions targets, but as it makes the transition to a developed economy, its status could be revised. India has called for a comprehensive, long-term monitoring network to accurately assess India's GHG inventory and its vulnerability and adaptation to environmental change (Government of India 2004). As part of this, India decides to establish fluxtowers (INDOFLUX) (Sundareswar et al. 2007) and the selection of suitable sites is in progress now. The challenge is how much spatial coverage flux towers can provide and how the measurements can be interpolated under diverse climatic, topographic and biotic gradients. Therefore, as a surrogate, it is essential to develop remote sensing based methodologies for rapid estimation of carbon flux which helps in the trade-off analysis in carbon budget and policy formulations for climate change mitigations.

Based on the above discussion, it could be concluded that 1). Operational monitoring of carbon flux is the hour of need, 2). The existing method for operational monitoring is widely criticized, 3). Approximately 50% carbon in terrestrial vegetation is located in tropical forest, 4). There is an overwhelming of studies in Neotropics whereas old world tropics is hardly represented, 5). Carbon estimates from Indian forests is not well studied though it is a mega-diversity country. By given that, the following sessions elucidate the existing attempts to estimate carbon flux in order to identify the best possible method in Indian context.

1.2. Review of the Literature

Three main approaches could be identified for estimating the carbon exchange: i) on-field measurement of biomass and its conversion to carbon (eg: Chave et al 2005, Ramachandran et al. 2007), ii). employment of physiological process-based models (Raich et al. 1991, Crammer et al. 1999), and iii) remote sensing based light use efficiency models (Xiao et al. 2004a, Olofsson et al, 2007a). Excellent reviews are available on the current status of these methods and their relative merits and demerits (Running et al. 2004, Hilker et al. 2006, Gibbs et al. 2007). The first approach is considered effective, however continuous measurements are difficult to achieve and may need destructive sampling at times. The second approach simulates ecosystem processes using detailed data sets obtained mainly from ground-based measurements like eddy covariance measurements. Though, high temporal resolution could be achieved, these models demands detailed inputs from a number of variables. Moreover, these measurements are made at single sites or across networks, but are not readily scaled up. Studies indicate that an advanced process-based model is not necessarily more accurate than remote sensing based light use efficiency models (Olofson et al. 2007b). Moreover, satellite-based measurements provide more than 30 years of global coverage with spatial resolution ranging from tens of metres to a few kilometres, and temporal sampling intervals of days to weeks. New sensors and satellites are expanding the scope of such observations.

Light use efficiency models assess canopy productivity based on Monteith's observation that gross primary productivity is proportional to amount of absorbed photosynthetically active radiation (APAR) and constant light use efficiency, ε (Monteith 1972, 1977).

$$\text{Gross Primary Productivity (GPP)} = \varepsilon * APAR$$

The method has been proven attractive to implement on the basis of remote sensing since it is possible to obtain these parameters from satellite. A number of studies (Ruimy et al. 1995; Field et al. 1995, Nemani et al. 2003, Olofson et al. 2007a) have used the light use efficiency model to estimate GPP at different spatial and temporal scales.

1.2.1 Light use efficiency (ε)

The value of light use efficiency (ε) was initially considered as relatively constant but substantial differences have been found that depend on ecosystem type, age, species composition, fertility and stresses (Ruimy et al. 1995, Lagergren et al. 2005), ε is therefore a crucial parameter to estimate. Broadly, there are two approaches to model ε from remote sensing; one is based on the environmental stress factors which restrict the carbon fixation and the other one is direct approach which tries to predict ε by measuring changes in leaf spectral reflectance resulting from photoprotection and chlorophyll fluorescence. Though, the second approach looks promising, its application is technically challenging at this moment as it involves sub-nanometer reflectance bands in the red and near infrared regions (often 690 and 760 nm) where solar radiation is not abundant due to atmospheric absorption (Meroni and Colombo 2006). Also, under natural sunlight illumination chlorophyll fluorescence emitted by the vegetation represents less than 3% of the reflected light in the near infrared part of the spectrum (Moya et al. 2004). At the same time, the studies based on environmental stress factors are much more developed and practically found feasible with present technology. Table: 1 summarise the present approaches to model LUE based on stress factors such as temperature, water, phenology, soil moisture, vapour pressure deficit and seasonality. Running et al. (1999) used temperature and water vapour deficit to model LUE in the standard MOD 17 A2/A3 product. Potter et al. (1999) modeled LUE as a function of temperature and moisture (water) stress scalars. Lagergren et al. (2005) derived LUE as a function of temperature and day of the year (seasonal factor). Xiao et al. (2004a, b) modelled LUE as a function of temperature, water and leaf phenology in the Vegetation Photosynthesis Model (VPM).

Table: 1. The structure of major light use efficiency models.

Model Name/Author	Model Logic	Reference
GLO-PEM	$\varepsilon = \varepsilon_0 . T . SM . VPD$	Prince and Goward (1995)
MODIS GPP	$\varepsilon = \varepsilon_0 . T . VPD$	Running et al (1999)
CASA	$\varepsilon = \varepsilon_0 . T . W$	Potter et al (1999)
VPM	$\varepsilon = \varepsilon_0 . T . W . P$	Xiao et al (2004)
Lagergren	$\varepsilon = \varepsilon_0 . T . DOY$	Lagergren et al (2005)
EC-LUE	$\varepsilon = \varepsilon_0 . T . SM$	Yuan et al (2007)

*Abbreviations are expanded in List of Abbreviations.

1.2.2 Absorbed photosynthetically active radiation (APAR)

APAR is the product of Incident PAR (IPAR) and fraction of photosynthetically active radiation (FPAR). IPAR is generally calculated by multiplying incident shortwave radiation by a constant value (0.45). The same is implemented in the standard MODIS product (MOD 17–Net Photosynthesis and Primary Productivity) (Heinsch et al. 2003). Recently, more advanced methods which take into consideration atmospheric conditions have been developed (van Laake and Sanchez-Azofeifa 2004 and 2005, Liang et al. 2006, Liu et al. 2008).

FPAR is the proportion of available shortwave radiation in the photosynthetically active wavelengths (0.4 to 0.7 mm) that a canopy absorbs. In remote sensing, it is usually estimated as a linear or non-linear function of NDVI due to its high correlation with NDVI (Ruimy et al. 1995, Olofsson et al. 2007). Many of the GPP models have directly substituted FPAR by NDVI values (FPAR ≈ NDVI) (Running et al 2004, Yuan et al 2007). But, there are clear cut evidences that NDVI is getting saturated in high biomass areas such as tropical forest (Huete et al. 2002, Glenn et al. 2008). In addition, its sensitivity to atmospheric conditions and soil background makes it less reliable in tropical environment. As an alternative, Enhanced Vegetation Index (EVI) was developed to account for residual atmospheric contamination (e.g., aerosols) and variable soil background reflectance (Huete et al. 1997, 2002). EVI directly normalizes the reflectance in the red band as a function of the reflectance in the blue band (Huete et al. 1997). A number studies shown that EVI is linearly related to FPAR and therefore, could be directly used as an estimate of FPAR (FPAR ≈ EVI) (Xiao et al. 2004a, b, 2005; Li et al. 2007, Mahadevan et al. 2008).

1.3. Profiling of Study Area

Western Ghats, specifically located in the western coastline of India, is one of the ‘hottest hotspots’ of biological diversity in the old world tropics. It contains more than 30% of all plant and vertebrate species found in India, in less than 6% of India’s landmass. Out of four thousand species of flowering plants known from the Western Ghats, 1500 are endemic (Nair and Daniel 1986). Due to varied topography and micro-climatic regimes, some areas within the region are considered to be active zones of speciation and localized centres of endemism (Blasco 1970, Nair and Daniel 1986). Anamalai Hills (administratively Indira Gandhi Wildlife sanctuary) located in the southern Western Ghats (Fig: 1) is one among them and is therefore considered as one of the 25 micro centres of diversity in the Indian Subcontinent (Nayar 1996). The western side of the hills is occupied by the luxuriant rainforest (humid forest), while the eastern side is dominated by dry forests. This is possibly due to the influence of south west monsoon which strikes the western part of the sanctuary first, and then advances eastwards, while retreats in reverse, creating a longer rainy period and shorter dry season length in the west. Also, the western side of the sanctuary is windward side of Western Ghats and therefore, the quantity of precipitation (mainly orographic rainfall) is higher at west whereas, precipitation is lower at east due to its leeward position. The overall terrain is hilly with the altitude ranging from 250m at the foothills in the north-east to 2500 m in the Grass Hills area in the south-west. The annual rainfall varies from 500 mm in the rain shadow eastern slopes to 5000 mm in the west. Mean daily temperature varies from <5^0 C in the winter at elevations above 2000m to nearly 40^0C in the eastern plain in the summer (Fig: 2).

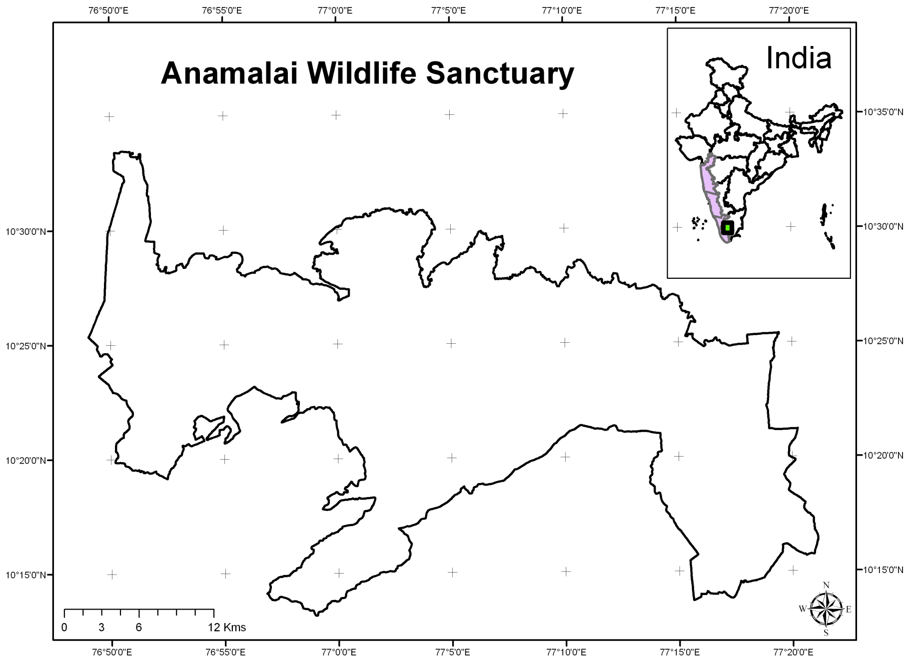

Fig. 1. Location map of Anamalai wildlife sanctuary in Western Ghats, India.

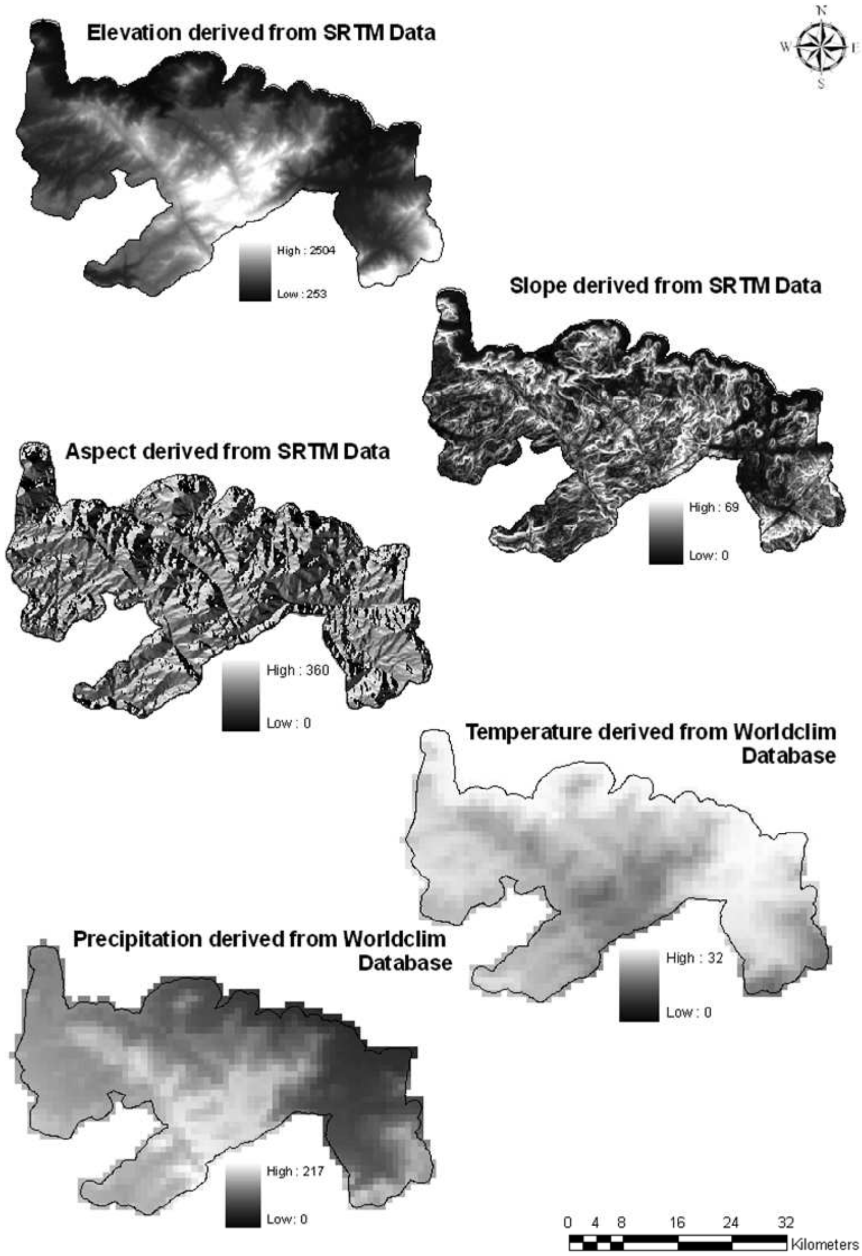

Fig: 2. Topographical (elevation (m), slope (degrees) and aspect (degrees)) and climatic gradients (temperature (^{0}C) and precipitation (cm)) in Anamalai wildlife sanctuary, India. Topographical variables are derived from SRTM (Shuttle Radar Topographic Mission) data and climatic variable are derived from 50 year average WorldClim datasets.

1.4. Formulation of Research Problem

Based on the above discussion, it could be inferred that the nature of the research problem is twofold; first one is related to heterogeneity (diversity) of the area at an aerial distance of 50 km and the second one is related to the input datasets in the present estimate by MOD 17A2 product.

1) Joseph et al (in press) identified seven major vegetation types in Anamalai hills using a satellite data of 24m resolution. Further studies using multivariate statistical techniques on ground based species data identified fourteen vegetation communities or species assemblages in the area. In such a diversified area, it may be point of interest to assess the performance of biome level classification of MODIS Land cover product (Since it is one of the most important inputs in MODIS GPP product) and its influence on the estimates of carbon assimilation rate.

2) By given that, LUE is a function of micrometeorological conditions and phenological properties of leaves, and NDVI is a function of amount of biomass, the GPP estimate given by MOD 17 A2 product (please note that climatic information is at a resolution of 1^{o} (≈ 100km) and FPAR (≈ NDVI) information at a scale of 1 km) may be vague estimation of the real GPP.

Therefore a better estimate of GPP is required with an alternative approach which takes into consideration of the heterogeneity area and local meteorological conditions.

1.5. Research Objective

1.5.1. General Objective

The aim of the study is to estimate GPP by considering the local environmental conditions and compare this estimate from MODIS GPP product. By doing so, the study will become an attempt to identify suitable methodology for the operational monitoring of carbon flux in tropical forests of India (It is worthwhile to mention here that remote sensing based light use efficiency model will be tested in the Indian forests for the first time). In addition, sensitivity analysis of each input variables in the GPP estimate in tropical forests will help to prioritise the future research needs.

1.5.2. Specific Objectives

The following specific objectives are formulated for addressing the above general objective.

- To estimate the Gross Primary Productivity of the area as a function of environmental and vegetation-type specific factors.

- To compare global level satellite-derived data products (MOD 17A2) with the estimate of GPP derived at the local scale by this study.

- To analyze the sensitivity of input variables and estimate its impact on carbon assimilation rate.

1.6. Research Questions

- Is advanced vegetation index such as EVI performing better than conventional vegetation index such as NDVI in tropical forest?

- Which MODIS water index can better represent ground soil moisture condition?

- How heterogeneity and seasonal changes in the vegetation types affect the carbon assimilation rate?

- What are the sensitive parameters in the GPP model? How it affects the total estimates of GPP.

- How global level data products behave at local scale? Is there any variation in MOD 17 A2 product when it is estimated at local scale? If yes, is it due to the algorithm difference or due to the changes in the resolution of the input datasets?

1.7. Hypotheses

Hypothesis 1

H_0 - Advanced vegetation index such as EVI can outperform conventional NDVI in biomass rich areas.
H_1 - Advanced vegetation index such as EVI can not outperform conventional NDVI in biomass rich areas.

Hypothesis 2

H_0 - MODIS Water index based on channels 6 can perform better than channel 5 to represent ground soil moisture conditions.
H_1 - MODIS Water index based on channels 6 can not perform better than channel 5 to represent ground soil moisture conditions.

Hypothesis 3

H_0 - The GPP estimate derived by the present study is not significantly different from MODIS GPP estimates.
H_1 - The GPP estimate derived by the present study is significantly different from MODIS GPP estimates.

1.8. Research Approach

The first step is to identify the environmental and vegetation type specific parameters for carbon assimilation. Based on available literature and expert knowledge, the parameters listed are maximum light use efficiency and its controlling factors (such as temperature (mainly in montane wet shola forest), water (rainshadow regions in the east) and longetivity of leaves (deciduous systems)), incoming PAR and fractional PAR. The second step is to identify the suitable data sources for estimating these parameters operationally. Four inputs identified are MODIS daily images, local weather observations, medium resolution remote sensing data and ground based biomass and soil moisture measurements. MODIS daily images could be used to derive vegetation and water indices which are further helped to calculate FPAR, water stress, and phenological stress; weather data could be used to estimate IPAR and temperature; medium resolution remotely sensed image could be used to derive land cover type and thereby assigning maximum light use efficiency to each land cover type; and ground based biomass and soil moisture data could be used to compare the MODIS derived indices. The third step is the selection of best indices in the model. For FPAR, two commonly used vegetation indices (NDVI and EVI) are available. For representing water stress, Land Surface Water Index (Xiao et al 2004) and Shortwave Infrared Water Stress Index (Fensholt and Sandholt 2003) (detailed descriptions are given in methods section) are available. Finally, carbon assimilated could be calculated as the product of maximum light use efficiency (controlled by environmental factors) and absorbed photosynthetically active radiation (another product of incoming PAR with fractional PAR). The modelled output can be compared with MODIS GPP product. A detailed sensitivity analysis could be useful for understanding the influence of each input parameter in the GPP estimate. Based on the experience, the challenges and uncertainties in each step can be discussed and suitable recommendations can be formulated for reducing the uncertainty in the operational monitoring of carbon flux in the Indian context.

2. Materials and Methods

2.1. Model Inputs

2.1.1. MODIS daily surface reflectance images

MODIS Surface Reflectance and radiance product (MOD02HKM) is a seven-band image computed from the MODIS Level 1A scans of raw radiance of bands 1 (620-670 nm), 2 (841-876 nm), 3 (459-479), 4 (545-565 nm), 5 (1230-1250 nm), 6 (1628-1652 nm), and 7 (2105-2155 nm). Channels 1 and 2 have 250 m resolution originally, but is aggregated to 500 m in this product and channels 3 through 7 have 500 m original resolution. Thus the entire channel data set is co-registered to the same spatial scale in the 500 m product. The radiance is in the unit of W/m2/µm/sr and reflectance is unitless values between 0.0 and 1.0. The MODIS L1B 500 m data are stored in the Earth Observing System Hierarchical Data Format (HDF-EOS) and typical file size is approximately 170 MB.

2.1.2. IRS P6 LISS III image

IRS P6 LISS III image (Indian Remote Sensing satellite) have a spatial resolution of 24 m and four bands (0.52 – 0.59, 0.62 – 0.68, 0.77 – 0.86 and 1.55 – 1.70µm). The raw data is in BIL (Binary Interleaved by Line) format and is geometrically uncorrected.

2.1.3. Meteorological Data

Four weather stations are available in and around the study area. These are located at different elevations ranges and represent four major vegetation types. The first station is located at an elevation of 450 m where thorn scrub forests are predominant, second station is located at an elevation of 700 m where deciduous forests are predominant, third station is located at an elevation of 1100 m where luxuriant evergreen forest grows and fourth station is located at an elevation of 2000 m where montane wet temperate (shola) forests-grassland system prevails. The parameters measured include total shortwave radiation, atmospheric temperature, precipitation, relative humidity, wind direction and wind speed.

2.1.4. Ground based biomass and soil moisture measurements

The quadrate data was available for the study area (Joseph et al. 2008). A stratified transect survey was conducted in the study area during the period of 2005-2006. The selection of strata was based on major vegetation types, different elevation ranges, and temperature and precipitation gradients. A circular plot of 10 m radius were laid on every 200 m interval along the transect length of 2 km. In each of the plot, all woody plants with ≥ 20 cm GBH (Girth at Breast Height, 1.3 m) were identified at species level, counted individuals and measured its height (hypsometer) and GBH using a tape. Biomass is derived from these datasets. Surface soil moisture data was available for one station in the study area.

In addition to the above, the following inputs are required for model comparison.

2.1.5. MODIS 12 Q1 Land cover product

MOD 12 Q1 Land cover product consists of five layers and each layer represents one classification system. These layers are IGBP global vegetation classification scheme, University of Maryland (UMD) scheme, MODIS-derived LAI/fPAR scheme, MODIS-derived Net Primary Production (NPP) scheme, and Plant Functional Type (PFT) scheme. The source data for the classification is coming from both Terra and Aqua satellites and the supervised decision-tree classification method is the classification technique. The latest version (*version:* 4) is for the year of 2004. The data are available in nominal 10-degree tiles in the Sinusoidal Grid projection with 1 km spatial resolution.

2.1.6. MODIS 15 A2 LAI and FPAR Product

The MOD15 A2 Leaf Area Index and Fraction of Photosynthetically Active Radiation absorbed by vegetation are 8 days composite provided at 1 km spatial resolution. The data is provided in EOS-HDF format and contains two bands; MODIS LAI_1km and MODIS FPAR_1km. The data type is unsigned 8-bit integer whose values ranges from 0 – 255. These MOD15 A2 data are provided as a level-4 composited product in Sinusoidal projection.

2.1.7. MODIS 17 A2 GPP Product

MODIS Terra Gross Primary Productivity 8-day Global 1 km SIN Grid V005 (MOD17A2) is a cumulative composite of net photosynthesis (PSN) values. The data is provided in EOS-HDF format and contains three bands; MODIS GPP_1km, MODIS PsnNet_1km and MODIS PsnQC_1km. Detailed description about the algorithm could be found in Heinsch et al. (2003) and Running et al. (2004). It requires daily inputs of incoming photosynthetically active radiation (IPAR), fraction of absorbed photosynthetically active radiation (FPAR), biome level maximum light use efficiency, minimum temperature over the 24 h period, and daytime average vapour pressure deficit. GPP is estimated for each 1 km^2 cell for each day of the year by first determining the absorbed photosynthetically active radiation (APAR). The incident PAR and the fraction of PAR that is absorbed by the vegetation (FPAR) determine APAR. Their product is multiplied by light use efficiency (ε) to get daily GPP. FAPAR for each 1 km cell is based on the spectral reflectances detected by the MODIS sensor (Myneni et al. 2002). The daily ε is based on a biome-specific maximum derived from a lookup table (Heinsch et al. 2003) and modified by scalars (0–1) associated with a daily minimum air temperature and vapour pressure deficit (VPD). The meteorological data are provided by the NASA Data Assimilation Office (DAO) based on a general circulation model run at the 1^o spatial resolution (~100 km). These MOD17A2 data are provided as a level-4 composited product in Sinusoidal projection.

2. 2. Model Framework

2.2.1. Calculation of Light use efficiency (ε)

For calculating LUE, four parameters were required; maximum light use efficiency of vegetation types, and its controlling factors such as temperature, water and longetivity of leaves (Evergreen vs. Deciduous). All these parameters are successfully formulated in satellite based Vegetation Production Model (VPM) and is validated in different vegetation types such as temperate evergreen needleleaf forest (Xiao et al 2004a), deciduous broadleaf forest (Xiao et al. 2004b), tropical moist evergreen forest (Xiao et al. 2005), alphine ecosysystems (Li et al. 2007) and a number of other biomes (Mahadevan et al. 2008). Therefore, the present study adopted the concept of VPM (Equation 1), though there were changes in the implementation.

$\varepsilon_g = \varepsilon_0 \cdot T_{scalar} \cdot W_{scalar} \cdot P_{scalar}$ ---------(1)

Where, ε_0 is the maximum light use efficiency, and Tscalar, Wscalar and Pscalar are the down-regulation scalars for the effects of temperature, water and leaf phenology on the light use efficiency of vegetation, respectively.

2.2.1.1. Maximum LUE (ε_0) - The values of maximum light use efficiency were taken from Biome-BGC model (White et al. 2000, Thornton et al 2002) after an extensive literature survey. Though there were scattered informations (Ruimy 1995, Xiao et al. 2004a,b), the Biome-BGC values were found to be most comprehensible which fit all the vegetation types in the study area. Moreover the values given by other estimates were not largely varying from Biome-BGC values. For example, Xiao et al (2005) adopted a value of 0.9765 g C/m^2/MJ IPAR from the studies of Malhi et al (1998) and Goulden et al. (2004) for tropical evergreen forests which is slightly lower than Biome-BGC value. The major vegetation type in the study area (according to Champion and Seth's classification for Indian Forests, Champion and Seth 1967), its corresponding Biome-BGC classification and maximum light use efficiency values are given in Table: 2. In absence of specific information about teak, the value deciduous broadleaf forest is assigned to teak (since it is a deciduous broadleaf tree) and for tea plantation, the value cropland is assigned.

Table: 2. The major land cover types in Anamalai Hills, corresponding Biome-BGC type and its maximum light use efficiency values

Major land cover type in the study area	Corresponding Biome-BGC vegetation type	ε_0 (g C/m^2/MJ IPAR)
West Coast Tropical Evergreen Forest	Evergreen broadleaf forest	1.159
Southern Montane Wet Temperate Forest	Evergreen broadleaf forest	1.159
Southern Tropical Deciduous Forest	Deciduous broadleaf forest	1.044
Southern Thorn Scrub	Closed shrubland	0.888
Grasslands	Grasslands	0.768
Teak plantations	Deciduous broadleaf forest	1.044
Tea plantations	Croplands	0.680
Agriculture and fallow lands	Croplands	0.680
Water bodies	Water bodies	0.000

2.2.1.2. Temperature scalar – Temperature control on photosynthetic process is represented as Tscaler and is calculated using the equation developed for the Terrestrial Ecosystem Model (Raich et al. 1991).

$$Tscalar = \frac{(T - T_{\min})(T - T_{\max})}{[(T - T_{\min})(T - T_{\max})] - (T - T_{opt})^2} \text{ ------------ (2)}$$

Where, T_{min}, T_{max} and T_{opt} are minimum, maximum and optimal temperature for photosynthetic activities. After careful examination of literature, the value of optimum temperature was taken as 28^0C (Tian et al. 1998, Ishida et al. 1999, Pons and Welschen 2003, Xiao et al. 2005).

***2.2.1.3. Water Scalar* –** In MODIS, there are two shortwave infrared channels, channel 5 (1230–1250 nm) and channel 6 (1628–1652 nm), which are wavelength areas at which leaf water content influence the radiometric response. Based on these channels, two water stress indices were derived in literature. Fensholt and Sandholt (2003) proposed two configurations of Shortwave Infrared Water Stress Index (SIWSI), which make use of normalized difference between NIR and Channel 5 in the first configuration and NIR and Channel 6 in the second configuration. Conversely, Xiao et al. (2004a, b) developed Land Surface Water Index (LSWI) based on NIR and Channel 6 which was primarily a repetition of the second configuration proposed by Fensholt and Sandholt (2003). For avoiding confusion in the present study, the first index, based on Channel 5, is called SIWSI (equation 3) and the second index, based on Channel 6, is called LSWI (equation 4). The selection of suitable index for the study area was based on the relative performance of these indices against the in-situ soil moisture data. Soil moisture data was available for one station in the study area. Correlation analysis showed that $LSWI_{6,2}$ is performing better than $SIWSI_{5,\ 2}$ and therefore Water scalar is calculated based equation (5) as proposed by Xiao et al. (2004a, b, 2005).

$$SIWSI_{(5,2)} = \frac{\rho_2 - \rho_5}{\rho_2 + \rho_5} \text{ --------- (3)}$$

$$LSWI_{(6,2)} = \frac{\rho_2 - \rho_6}{\rho_2 + \rho_6} \text{ ---------- (4)}$$

Where, ρ_2 is the surface reflectance at NIR band and ρ_5 and ρ_6 are surface reflectance at SWIR bands. The values range from -1 to +1, and the simple formulation of Wscalar is a linear scalar with a value range of 0 to 1.

$$Wscalar = \frac{1 + LSWI}{1 + LSW\,\mathrm{Im}ax} \text{ -------- (5)}$$

Where, $LSWI_{max}$ is the maximum LSWI value within the photosynthetically active period.

***2.2.1.4. Phenological scalar* –**Pscalar is dependent upon life expectancy (longevity) of leaves (deciduous versus evergreen). In the study area, leaves were retained throughout the wet season and therefore Pscalar is taken as 1 during this season. For the dry season, Pscalar is calculated using the equation (6) developed by Xiao et al. (2004a, b, 2005) for their VPM model.

$$Pscalar = \frac{1+LSWI}{2} \text{ ------------- (6)}$$

2.2.2. Computation of Absorbed Photosynthetically Active Radiation (APAR)

For estimating Absorbed Photosynthetically Active Radiation (APAR), two inputs were required. First one is the Incident PAR (IPAR) and the second one is the fraction of absorbed PAR (FPAR) (equation 7).

$$APAR = IPAR \cdot FAPAR \text{ ------------ (7)}$$

2.2.2.1. Incident Photosynthetically Active Radiation (IPAR) - Generally, IPAR is calculated as 50% (specifically 0.45) of the total solar radiation. When enough ground observations are not available, IPAR is modelled as a function of total shortwave radiation at the top of the atmosphere (TOA) and the atmospheric conditions which decide the amount of radiation to reach at the ground level. A number of such algorithms are available in the literature (van Laake and Sanchez-Azofeifa 2004, 2005, Liang et al. 2006, Liu et al. 2008). Since, enough numbers of weather stations are available in the study area; the present study did not attempt any of these methods. Therefore, IPAR is calculated using the equation (8) in similar to MOD 17 A2 product (Heinsch et al. 2003).

$$IPAR = SWRad \cdot 0.45 \text{ ----------- (8)}$$

2.2.2.2. Fraction of Photosynthetically Active Radiation (FPAR) – Many models and studies have used vegetation indices values as a substitution for FPAR due to their high correlation. Running et al. (2004) and Yuan et al. (2007) used NDVI for FPAR while Xiao et al. (2004a, b, 2005), Li et al. (2007) and Mahadevan et al. (2008) used EVI for FPAR. Therefore, both the approaches were attempted in the present study. NDVI and EVI were calculated using the equations (9) and (10) respectively. Then the selection of index for the model was based on their relative performance against the ground biomass. For this purpose, biomass was calculated using allometric equations developed for Western Ghats (Murali et al. 2005). Two allometric equations were used. One was for evergreen forests (equation 11) and the other was for deciduous forests (equation 12). The Basal Area required for these equations is calculated from GBH using the equation (13). The values of biomass were plotted against the corresponding vegetation indices values and the coefficient of determination (R^2) was noted. EVI has shown better R^2 than NDVI and therefore the values of EVI were substituted for FPAR in the model.

$$NDVI = \frac{\rho_{nir} - \rho_{red}}{\rho_{nir} + \rho_{red}} \text{ ----------------- (9)}$$

$$EVI = G * \frac{\rho_{nir} - \rho_{red}}{\rho_{nir} + (C1 * \rho_{red} - C2 * \rho_{blue}) + L} \text{ ---------------- (10)}$$

Where ρ_{nir}, ρ_{red} and ρ_{blue} are surface reflectance values at NIR, Red and Blue bands respectively, G is the gain factor, C1, C2 are the coefficients of the aerosol resistance term, which uses the blue band to correct for aerosol influences in the red band, and L is the canopy background adjustment that addresses non-linear, differential NIR and red radiant transfer through a canopy. For MODIS, the values are set to be G=2.5, C1=6, C2=7.5 and L=1.

$$Biomass\_Evergreen = [-2.81 + 6.78 \cdot BasalArea] \qquad (r^2 = 0.53) \text{ ------------ (11)}$$

$$Biomass\_Deciduous = [-73.55 + 10.73 \cdot BasalArea] \qquad (r^2 = 0.82) \text{ ---------(12)}$$

$$BasalArea = \frac{(GBH)^2}{4\pi} \text{ ------------- (13)}$$

2.2.3. Computation of Gross Primary Productivity (GPP)

The estimation of Gross Primary Productivity was done as the cross product of light use efficiency with Absorbed Photosynthetically Active Radiation (equation 14). The complete model is given in equation (15).

$$\text{Gross Primary Productivity (GPP)} = \varepsilon \cdot APAR \text{ --------- (14)}$$

$$\mathrm{GPP} = (\varepsilon_0 \cdot Tscalar \cdot Wscalar \cdot Pscalar) \cdot (IPAR \cdot FPAR) \text{ ------------ (15)}$$

2.3. Model Implementation

2.3.1. Generation of maximum light use efficiency map

Since maximum light use efficiency is a vegetation specific factor, creation of an accurate land cover map was the first step. It was done through supervised classification of the IRS P6 LISS III data. The image was acquired from National Remote Sensing Center (NRSC), Hyderabad, India. The image was geometrically corrected with respect to Enhanced Thematic Mapper (ETM+) data based on I^{st} order polynomial regression between ground control points (RMSE<0.5 pixel) to compute the coefficients for two co-ordinate transformation equations, and registered to the UTM projection. Based on the knowledge of the data and ground truth information, nine different land cover classes were identified in the study area. Parametric signatures were used to train a statistically based (e.g. mean and covariance matrix) classifier to define the classes. Training sites were digitized within ERDAS Imagine (ERDAS 2006), using the AOI tools. The inquire cursor was used to identify a single pixel (seed pixel) that represents the training sample then neighbors to the seed pixel were added to the training sites. After several iterations with different criteria, the maximum size of area (geographic constraints) and spectral Euclidian distance were limited to 500 pixels and 10 respectively. After the signatures were defined, the image was classified using the maximum likelihood parametric rule. An accuracy assessment was performed by comparing the classified image with reference data, collected from the field survey. Upon completion of this step, the values maximum light use efficiency which has taken from Biome-BGC Model (Table: 2) were assigned to each land cover type.

2.3.2. Generation of Wscalar, Pscalar and FPAR

Daily MODIS surface reflectance images (MOD02HKM – Level 1B calibrated Radiance – 500m) were downloaded from data distribution centre of Goddard Space Flight Centre, NASA (http://ladsweb.nascom.nasa.gov/) for a period of two years (September, 2006 – August 2008). The data were projected into Universal Transverse Mercator (UTM) Projection and reflectance images were extracted using MODIS Conversion Tool Kit (MCTK) – a plug-in associated with ENVI/IDL software environment (http://www.ittvis.com/). Since MCTK user interface can handle only one image at a time, suitable programs were written in IDL language for automating the work. The georeferenced images were subsetted using the study area boundary. Water indices (SIWSI and LSWI) were calculated for each image using equations (3) and (4) respectively. Similarly, Vegetation indices (NDVI and EVI) were calculated as per equations (9) and (10) respectively. The correlation between water indices and soil moisture data were carried out for selecting the suitable index. Subsequently, Wscalar and Pscalar were calculated using equations (5) and (6) respectively. For selecting the suitable index to represent FPAR, the values of vegetation indices were plotted against biomass values. The biomass of sample plots were calculated using equations (11) and (12) depending on the type of vegetation. The coefficient of determination (R^2 - value) was the criteria for selection. Since the number of images were enormous (2 years of daily images), it was not possible to do the work manually. Therefore, suitable programs were made in Python (*ver*.2.5) scripting language for automating the work.

2.3.3. Generation of Tscalar and IPAR

Daily temperature and IPAR values were collected from weather stations. Since these observations were collected from point locations, it was necessary to extrapolate the observations to study area. This was done by taking into consideration of long term climatic data (50 year average global climatic datasets from WORLDCLIM) (Hijmans et al. 2005) and altitudinal variation in the study area. The digital elevation model was placed over climatic data to study the changes in climatic parameters with respect to elevation. Four zones were digitized by assuming that the first weather station is a representative of first zone, second weather station is a representative second zone and so on. The altitude of weather station, its extrapolated range and major vegetation type in the zone are given in Table: 3. The zones were digitized and new attribute columns were generated for Tscalar and IPAR. The Tscalar and IPAR, calculated using equations (2) and (8), were entered in their respective attribute columns and rasterized to generate daily Tscalar and IPAR images.

Table: 3. The altitude of weather station, its extrapolated range and major vegetation type in the zone.

Altitude of Weather Stn (m)	Extrapolated Range (m)	Major vegetation type around the station
450	280 – 600	Southern Thorn Scrub
700	600 – 1000	Southern Mixed Deciduous Forest
1100	1000 – 1600	West Coast Tropical Evergreen Forest
2000	1600 - 2504	Southern Montane Wet Temperate Forest

2.3.4. Calculation of LUE, APAR and GPP

LUE, APAR and GPP were calculated using equations (1), (7) and (14) respectively. Since, Pscalar is a season-specific parameter, defining of season was necessary during LUE calculation. This was done by plotting the monthly variation in temperature and precipitation in 50 years time period (WORLDCLIM datasets). Finally, GPP was calculated as the cross product of LUE and APAR. From the daily GPP images, five points were randomly selected for each vegetation types. The average of these values was considered as GPP of that vegetation type for further analysis.

2.4. Model Comparison

MODIS Terra Gross Primary Productivity 8-day Global 1km SIN Grid V005 (MOD17A2) products were downloaded from Land Processes Distributed Active Archive Centre (LP DAAC) (http://edcimswww.cr.usgs.gov/pub/imswelcome/) for the study period (September 2006 to August 2008). The images were reprojected to UTM projection and the first band, i.e., GPP_1km, was extracted. These scaled digital images were converted into biophysical quantity using the equation (16).

$$\text{Biophysical pixel} = \text{scale factor} \cdot \text{digital value} \cdot 1000 \quad \text{-----------(16)}$$

where biophysical pixel is sequestered carbon (kg C/m^2), scale factor is the gain for the MODIS productivity products (0.0001), digital value is the numeric value of a file pixel, and 1000 is the conversion factor from kilogram to gram.

In a similar fashion, the daily GPP estimates from the present study were composited into 8-day cumulative composite. Before compositing, all the images were resampled to 1 km resolution for valid comparison. The pixels from the same geographical locations were picked up in both the images (GPP images by the present study and MODIS GPP images). Five points were selected for each vegetation types and every fifth composite were included in the analysis. Subsequently, Paired sample t-test was conducted to check whether the GPP calculated with the present study is significantly different from MODIS GPP.

Further investigations were carried out to understand the difference between the algorithms of the present study and MOD 17A2 product. MODIS GPP product heavily depends on MODIS land cover product (MOD 12Q1) through the use of BPLUT (Biome Parameter Look-Up Table). Therefore, the accuracy of this product was the first step to be estimated in the comparison. The MOD 12 Q1 land cover product for the study area was downloaded from LPDAAC server. The downloaded data is reprojected to UTM projection and subsetted with the study area. The second layer from the land cover product was extracted since MOD 17 uses the UMD classification system. The accuracy of the product was checked using 225 ground control points collected from the field.

In addition, MOD 17 A2 GPP algorithm (equation 17) is implemented using the ground data to know whether the difference in the estimate is due to the formulation of the model or due to the changes in the resolution of the input data. The required parameters were

i. ε_0 - The maximum light use efficiency
ii. TMINmax - The daily minimum temperature at which $\varepsilon = \varepsilon_0$ (for optimal VPD)
iii. TMINmin - The daily minimum temperature at which e = 0.0 (at any VPD)
iv. VPDmax - The daylight average vapour pressure deficit at which $\varepsilon = \varepsilon_0$ (for optimal TMIN)
v. VPDmin - The daylight average vapour pressure deficit at which $\varepsilon = 0.0$ (at any TMIN)
vi. IPAR - Photosynthetically Active Radiation incident on the vegetative surface
vii. FPAR – Fraction of Photosynthetically Active Radiation that canopy absorbs

The two parameters for TMIN and the two parameters for VPD are used to calculate the scalars that attenuate ε_0. These scalars were derived as simple linear ramp functions as illustrated in Fig: 3.

$$\text{GPP} = (\varepsilon_0 * TMIN\_scalar * VPD\_scalar) * (IPAR * FPAR) \text{ ------------- (17)}$$

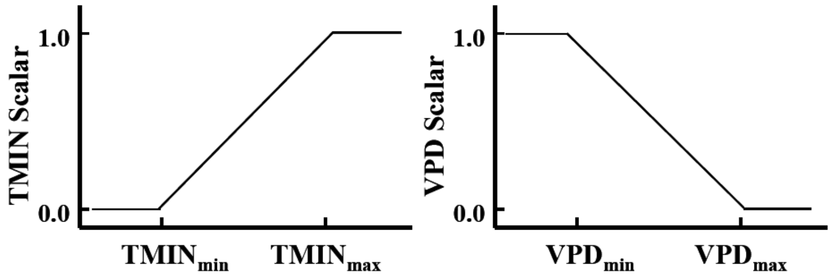

Fig: 3. The TMIN and VPD attenuation scalars are simple linear ramp functions of daily TMIN and VPD.

All these parameters except FPAR were calculated using data which were available at the local scale (in-situ data). Vapour Pressure Deficit was calculated from saturation vapour pressure and relative humidity using equation (18).

$$VPD = SVA * \frac{(100 - R.H)}{100} \text{ ----------- (18)}$$

Where, SVA is the saturation vapour pressure of air at a particular temperature and R.H is the relative humidity at that temperature.

Since ground measured FPAR was not available, it was derived from MOD 15 A2 LAI/FPAR product. The datasets were downloaded from LPDAAC server, reprojected to UTM projection, subsetted with study area and extracted the FPAR values.

2.5. Model Sensitivity

The sensitivity of each input variables in the total GPP estimate were analysed. The selected variables are temperature scalar, water scalar, phenological scalar, incident

PAR and fractional PAR. Maximum light use efficiency was not selected for the sensitivity analysis since it is a biome specific constant. The yearly mean and standard deviation of input variables were calculated. The values of standard deviation were altered by ±10% repeatedly for each variable while keeping the other variables constant and the corresponding change in GPP was noted.

3. Results

3.1. Vegetation type and maximum LUE (ε_0) maps

Vegetation and land cover type mapping using the IRS P6 LISS III data showed the area is dominated by deciduous forest (487.6 km^2) and evergreen forest (230.2 km^2) (Fig: 4). The nine land cover classes, their area statistics and estimated classification accuracy are given in Table: 4. The pristine grasslands, a particular feature of the hills covered an area of 86 km^2. In addition to natural vegetation types, the other land cover types in the area are plantations, agriculture areas and reservoirs. Overall classification accuracy was 83% and the Kappa statistic was 0.79. Each of these vegetation types were assigned by the maximum light use efficiency values according to Biome-BGC model.

Fig: 4. Major land cover types in Anamalai hills, India derived from IRS P6 LISS III satellite data.

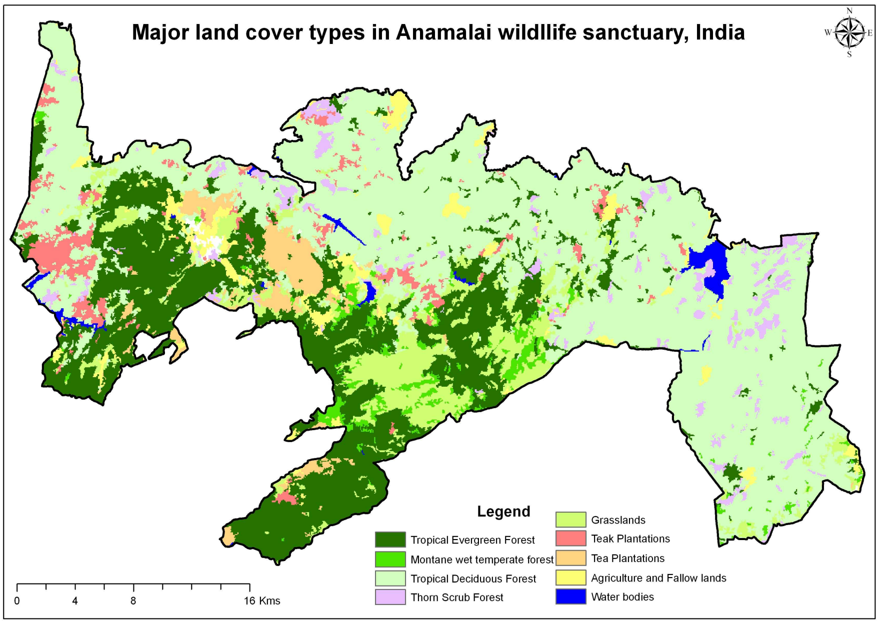

Table: 4. Area statistics of major land cover types and their classification accuracy in Indira Gandhi Wildlife Sanctuary, India (Area statistics is derived from the IRS P6 LISS III data dated 28th March, 2006).

Sl. No.	Land cover Type	Area (Sq.km)	Area (%)	Producer Accuracy	User Accuracy
1	Tropical Evergreen Forest	230.2	23.8	87.5%	89.4%
2	Montane wet temperate forest	21.8	2.2	66.7%	83.3%
3	Tropical Deciduous Forest	487.6	50.3	90.0%	75.9%
4	Thorn Scrub Forest	34.3	3.5	58.8%	76.9%
5	Grasslands	85.8	8.9	70.0%	95.5%
6	Teak Plantations	31.3	3.2	75.0%	69.2%
7	Tea Plantations	30.2	3.1	100.0%	84.6%
8	Agriculture and Fallow lands	36.5	3.8	84.6%	91.7%
9	Water bodies	10.9	1.1	100.0%	90.0%
	Total Area	968.6	100.0		

Overall Classification accuracy - 82.67%

Overall Kappa statistics - 0.79

3.2. Tscalar, Wscalar and Pscalar

Study on temperature, water and phenological parameters indicated that all these parameters have spatial and temporal dimensions. Temperature was a constraint in higher altitude areas where montane wet temperate forest (shola forest) – grassland system is existing. Eastern plains in the study area (rainshadow regions) where deciduous and thorn scrub forests are predominant, temperature was not a limiting factor. The correlation analysis between water stress indices and soil moisture data indicated that MODIS channel based on 6^{th} band (LSWI) is performing better than 5^{th} band (SIWSI). The correlations were 0.71 and 0.64 respectively (Table: 5). Therefore, LSWI was taken for calculating Wscalar and Pscalar. For incorporating phenological scalar into the model, it was necessary to define wet and dry seasons. Fig: 5 shows the variation in temperature and precipitation in the study area in different months. Precipitation showed a sudden increase during the month of June. The highest amount of precipitation was observed during the month of July. In December, the intensity has substantially reduced, more than half from previous month (170 mm in November to 69 mm in December). In case of temperature, June has showed a drastic decrease in temperature in similar to precipitation. Therefore, the wet season is defined as the period between June to November (Julian Days 152 to 333) and dry season is defined as the period between December (Julian Day - 334) to May (Julian Day - 151). During the period of wet season, the Pscalar is not considered as a constraint for carbon assimilation and therefore included in the model.

Table: 5. Correlation analysis between soil moisture data and water stress indices. MODIS channel based on 6th band (LSWI) has shown better correlation than 5th band (SIWSI).

	LSWI ($MODIS_{6,2}$)	SIWSI ($MODIS_{5,2}$)
Correlation coefficient	0.71	0.64

Fig: 5. Variation in monthly temperature and precipitation in Anamalai hills of Western Ghats, India (Data Source: WORLDCLIM 50 year average)

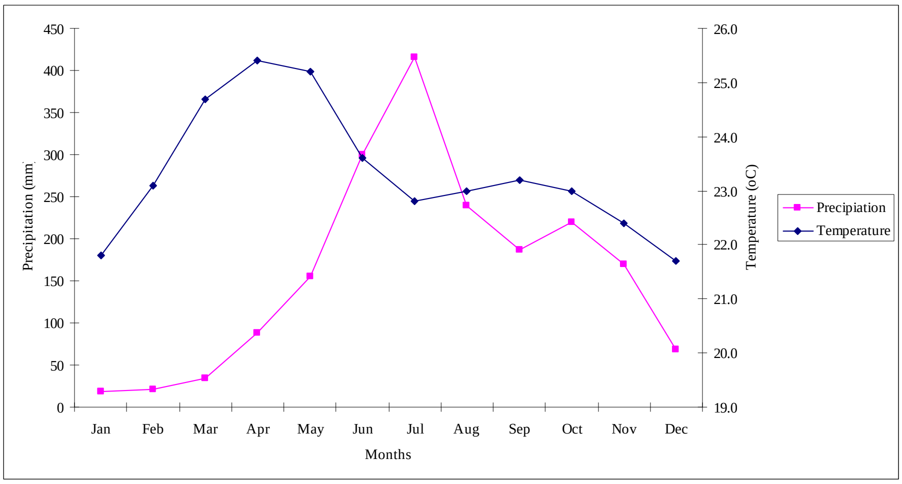

3.3. Light use efficiency (ε)

Since the carbon assimilation is a vegetation and season specific property, all the results are categorised into season-wise in addition to yearly average. In the yearly estimate, the values of light use efficiency varied from zero to 0.577 g C/m^2/MJ (Fig: 6). The maximum light use efficiency is observed in those areas where there are no physical constraints. Phenologically, these areas are dominated by evergreen forests within an altitudinal range of 800 – 900 m. The average temperature is around 26^{0}C, a value which is slightly less than the optimum temperature (28^{0}C) considered. A number of rivulets in the area ensure the abundance of water in the physiological processes. The lowest values are observed in mountain grasslands and shola forest systems where temperature is the most important constraint. Moreover, the ε_0 fixed for grasslands was lower. In dry season, the higher elevation rainforests (> 1200 m) is showed a better LUE than wet season. This is in agreement with the changes in temperature in both seasons. The lower value of LUE in deciduous-scrub system in dry season was due to the water and phenological stresses. In wet season, the deciduous-scrub system showed higher values of LUE due to the absence of limiting factors in physiological processes.

3.4. Incident PAR

The average annual IPAR was higher at eastern plains of the study area (station 3 and 4) and lower at higher elevation western ranges (station 1 and 2) (Table: 6). In dry season, there was not much variation in the incoming PAR among the stations, whereas this difference was prominent in wet season. From station-1 to station-4, the difference was almost double. The positive correlation between elevation and solar radiation (increase in solar radiation with respect elevation) is not found significant in the study area. This is mainly because of the dense cloud cover over the western high ranges during the wet season. In terms of vegetation types, the eastern plain is dominated by deciduous and thorn scrub forest formations and the western high ranges are dominated by evergreen-shola forest formations.

Table: 6. The variation in average IPAR (MJ/m^2) in different weather stations in the study area.

Average IPAR	Station No.			
	Station-1	Station-2	Station-3	Station-4
Yearly average	6.86	6.69	8.04	8.43
Dry season	8.75	8.33	9.56	9.01
Wet season	4.96	5.05	6.51	7.85

Fig: 6. The variation in light use efficiency (g C/m^2/MJ APAR) in Anamalai Hills of Western Ghats, India. a. Yearly average. b). dry season average and c). wet season average

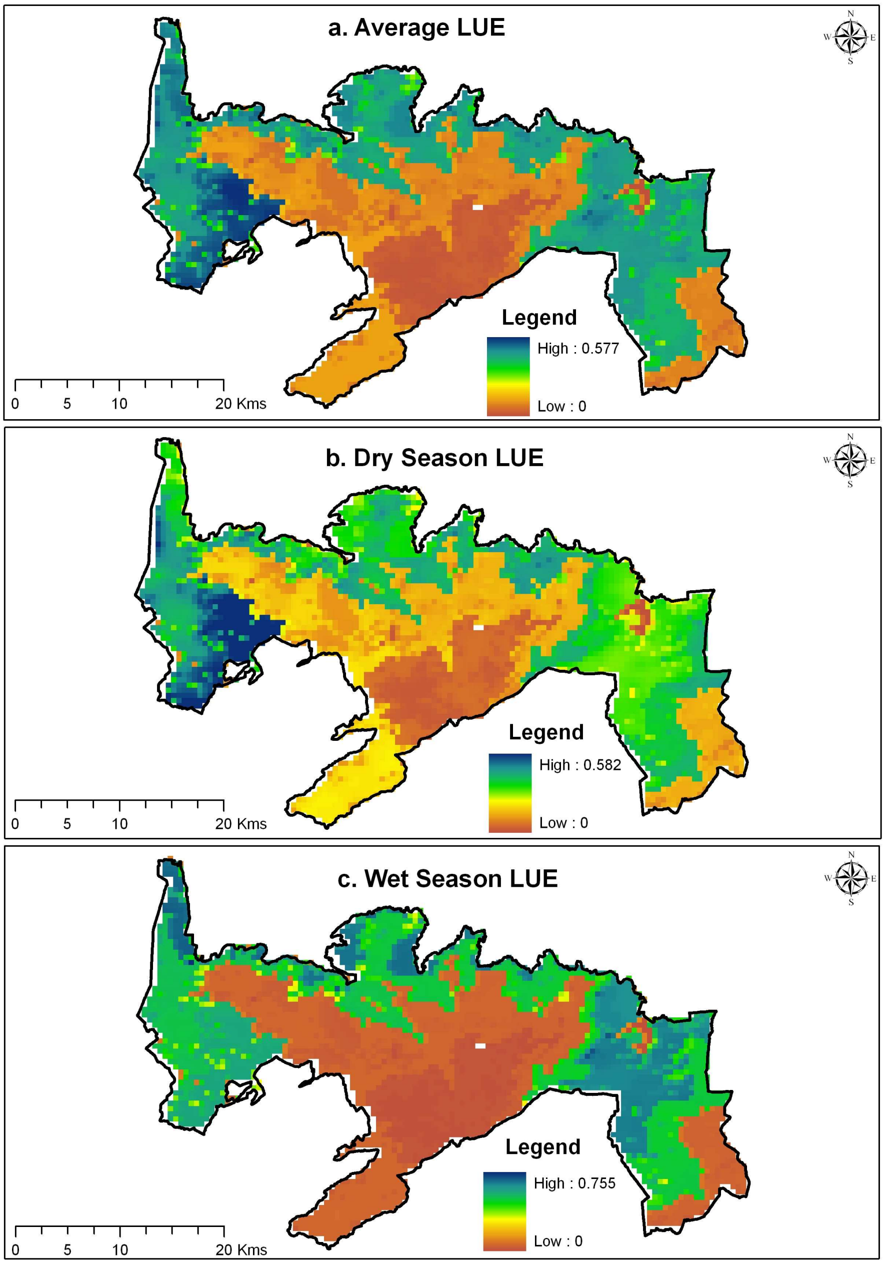

3.5. Fractional PAR

The estimation of fractional PAR was based on the relationship between vegetation indices and biomass of sample plots. Biomass calculated using allometric equations for different vegetation types were varied from 14 to 515 tons/ha with an average of 148±130 tons/ha. For evergreen vegetation types, the average biomass per hectare was 233±132 tons while in deciduous, it was 76±66 tons. The NDVI values ranged from 0.33 to 0.66 with an average of 0.45 while EVI vary from 0.23 to 0.53 with an average of 0.33. A good positive relation was found between vegetation indices and biomass of both the vegetation types. Enhanced Vegetation Index (Fig: 8) performed slightly better Normalized Differential Vegetation Index (Fig: 7) in both the vegetation types. The coefficient of determination (R^2) between EVI and biomass was 0.47 for evergreen forest and 0.39 for deciduous forest. For NDVI, the values were 0.38 and 0.34 respectively. Therefore, EVI was taken as FPAR in the model.

3.6. Gross Primary Productivity

The high values of GPP are observed in the low elevation rainforests followed by deciduous system in the western part of the sanctuary (Fig: 9). The montane grasslands are showed the poor carbon assimilation capacity primarily due to the unavailability of optimum temperature and enough IPAR. Most of the montane areas are cloud covered throughout the day especially in wet season which limits the IPAR to reach the ground. The relative higher value of GPP in the shola forest in these mountain areas in dry season is an additional evidence to cloud problem. Seasonal variation in carbon assimilation was very prominent in the study area. The low elevation evergreen forests is observed higher carbon assimilation in dry season while deciduous-scrub forests is showed higher carbon assimilation in wet season. During the dry season, the water and phenological stresses are prevalent in deciduous system. This might have limited the conversion of IPAR into GPP, though IPAR was abundant. In wet season, there are no physical constraints in deciduous systems which enables the luxurious leaf growth and thereby carbon assimilation.

With respect to vegetation types, deciduous forest and teak plantations (another deciduous tree) showed higher carbon assimilation rate especially in wet season (Fig: 10). In dry season, the evergreen forest showed higher assimilation rate. Even in same phenological category, the assimilation rate was different. There are two types of evergreen forest observed in the study area, first one is found at an elevation range of 700 – 900 m and the second one is found at a range of 1100 – 1500 m. Both the areas showed a significantly different assimilation rate. If low elevation rainforest is alone considered, the carbon assimilation rate is highest in this forest type whereas, if both are considered together, the values match more or less similar with deciduous forests. The low values of GPP were observed for grasslands and tea plantations.

Fig: 7. Biomass-NDVI relation in Evergreen and Deciduous vegetation types in Anamalai hills, Western Ghats, India

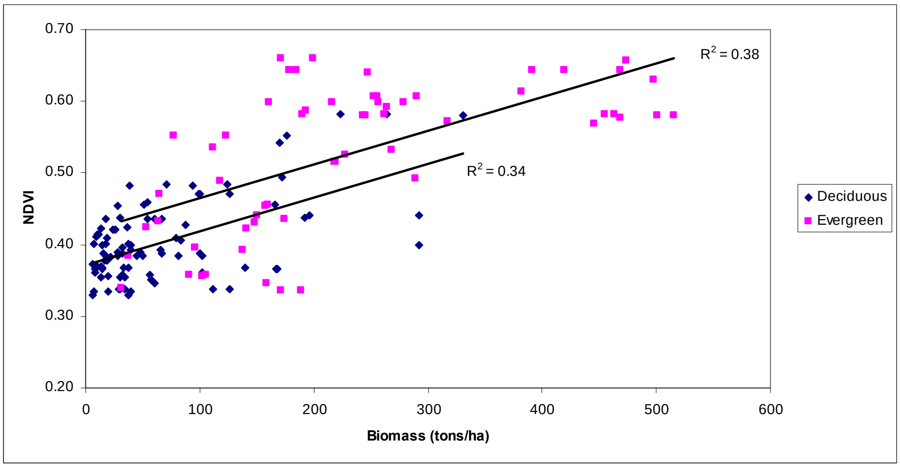

Fig: 8. Biomass-EVI relation in Evergreen and Deciduous vegetation types in Anamalai hills, Western Ghats, India

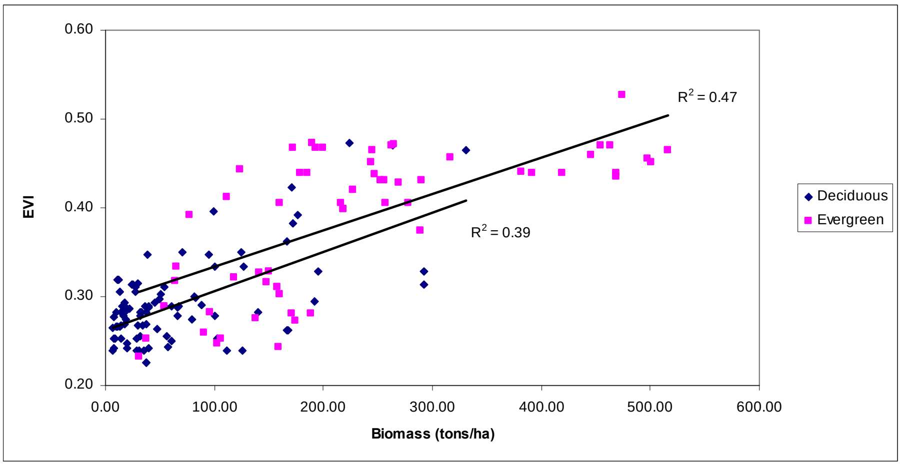

Fig: 9. The variation in carbon assimilation rate (g C/m^2/day) in Anamalai hills of Western Ghats, India. a). Yearly average. b). Dry season average and c). Wet season average

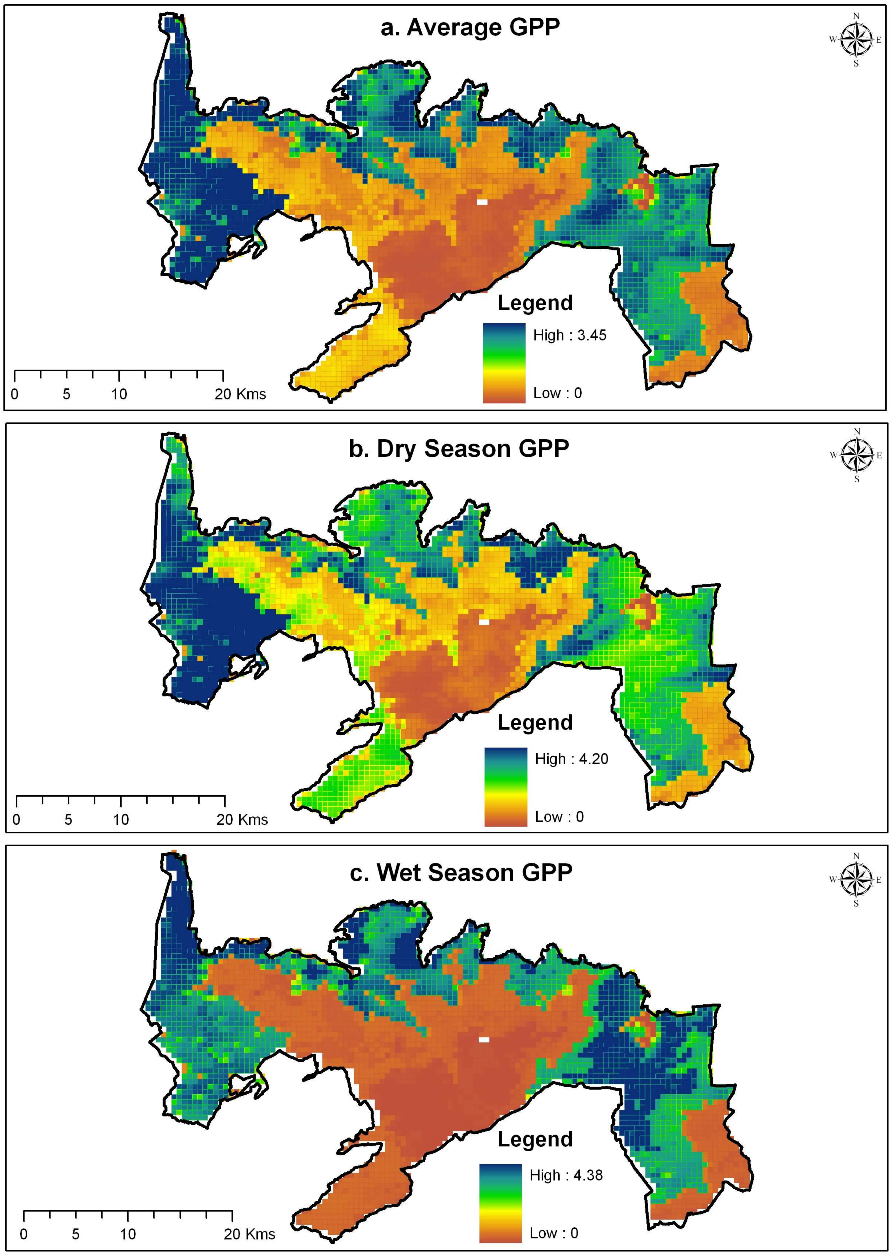

Fig: 10. Carbon assimilation rate (g C/m^2/day) in different vegetation types in Anamalai Hills of Western Ghats, India.

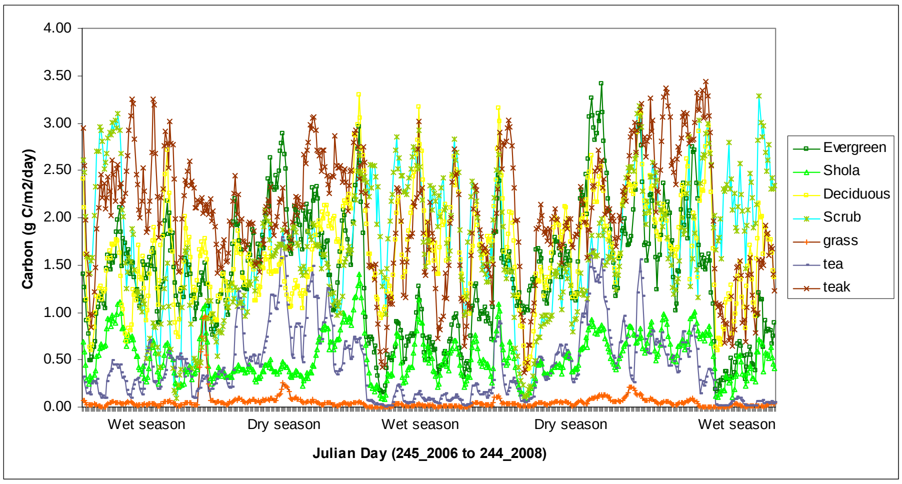

3.7. Model Comparison

Comparison of 8-day cumulative composite between the GPP estimated by the present study and the GPP estimated by MODIS 17A2 product is given in Table: 7. On an average, the estimate by the present study was nearly half from the MODIS product. The paired sample t-test confirmed that means are significantly different at 95% confidence limits ($p < 0.000$) (Table: 8).

Table: 7. Basic statistics (minimum, mean, maximum and standard deviation) of 8-day cumulative composite by the present study and MODIS 17A2 GPP product

		Min	Mean	Max	SD
GPP estimated by the present study	Yearly Average	1.37	12.93	30.54	7.17
	Dry Season	1.35	12.86	36.64	6.53
	Wet Season	1.16	12.85	39.21	8.85
MODIS GPP estimate	Yearly Average	4.91	30.23	50.83	11.34
	Dry Season	4.43	38.02	63.41	17.36
	Wet Season	5.14	22.45	46.91	7.23

Table: 8. Comparison of GPP estimated by the present study (GPP_ESTMD) with the MODIS 17A2 GPP product using Paired sample t-test

Paired Parameter	Paired Differences			t	df	Sig. (2-tailed)
	Mean	Std. Deviation	Std. Error Mean			
GPP_ESTMD - MODIS_GPP	11.54	16.34	0.79	14.55	423	0.00

The difference in the GPP estimates was analysed by comparing the input variables. Since maximum LUE is a BPLUT property, the accuracy of the land cover map used in both models was the primary concern. The assessment of MODIS land cover map for the study area indicated that 50% of the forests belong to evergreen category in contrast to 24% in the present study. The land cover type, area statistics and accuracy assessment are given in Table 9. It was surprised to note that 20% of the deciduous forest is mapped as crop land in MODIS land cover product (Fig: 10). The classes such as evergreen needleleaf forest, woody savanna (grassy woodland) and savanna are practically not found in the Anamalai hills whereas MOD 15 A2 mapped these classes as 22% of the total area. The major vegetation type in the area (50% according to present study), i.e., deciduous broadleaf forest, was underrepresented (0.4%) in the MODIS land cover product. The accuracy estimation using 225 ground control points indicated that MODIS land cover product has an overall accuracy of 46% with kappa coefficient of 0.34.

The implementation of MODIS 17 A2 algorithm using the ground measured data indicated that the algorithm difference between the present study and the MODIS product is not the reason in the changes in GPP estimate. Both these models were given more or less similar results. The changes in the result are given in Table: 10. Sometimes, globally derived results (gloabal datasets of 1^0 resolution) were three times higher than the locally derived outputs. For example, the present study and MOD 17 A2 algorithm using in-situ data resulted a carbon assimilation rate of 12.8 and 11.6 g C/m^2/8 days respectively, whereas, globally derived datasets yielded a value of 42.8 g C/m^2/8 days. In terms of vegetation types, locally derived models showed that evergreen, deciduous and teak plantations assimilate carbon at higher rate, and grassland and tea plantations assimilates at lower rates. Globally derived outputs showed that evergreen and tea plantations absorb carbon at higher rate, and scrub forest and grasslands absorb at lower rates. The tea plantations are mapped as evergreen forest in MODIS land cover product and this may be reason for higher assimilation rate of tea. In terms of season, the present study showed that deciduous types (deciduous forest, scrub forest and teak plantations) has higher assimilation rate in wet season and low assimilation rate in dry season. In contrary, MOD 17A2 model (both local and global datasets) showed that deciduous types has higher assimilation rate in dry season and lower assimilation rate in wet season. The present study algorithm include a phenological factor (Pscalar) whereas, the MOD 17 A2 algorithm does not include a specific phenological measurement. The estimation of higher carbon assimilation for deciduous types in dry season by MOD 17 A2 algorithm was not found logical since leaves were nearly absent during the season. For evergreen types (evergreen forest, shola, grassland and tea plantation), all the models were showed higher carbon assimilation in dry season and lower assimilation in wet season.

Fig: 11. Major land cover types in Anamalai hills, India according to MODIS Land cover product (MOD 12Q1)

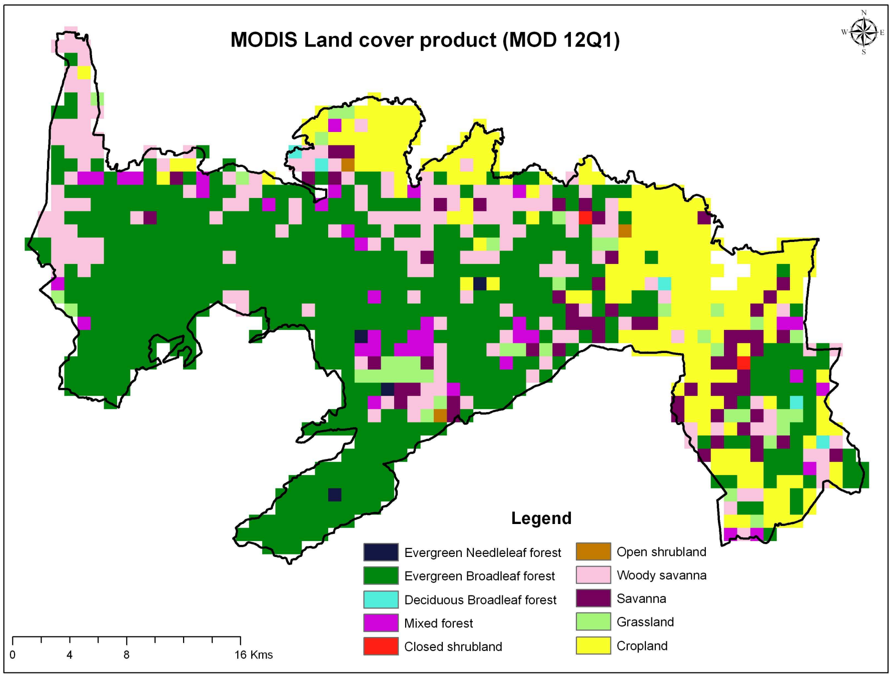

Table: 9. Area statistics of major land cover types and their classification accuracy in Indira Gandhi Wildlife Sanctuary, India (Area statistics is derived from the MODIS Land cover product MOD 12Q1).

Sl. No.	Land cover Type	Area (Sq.km)	Area (%)	Producer Accuracy	User Accuracy
1	Evergreen Needleleaf forest	3.5	0.4	0.0%	0.0%
2	Evergreen Broadleaf forest	486.7	50.8	87.5%	80.2%
3	Deciduous Broadleaf forest	4.2	0.4	3.1%	66.7%
4	Mixed forest	33.5	3.5	27.3%	66.7%
5	Closed shrubland	1.6	0.2	28.6%	80.0%
6	Open shrubland	2.7	0.3	0.0%	0.0%
7	Woody savanna	149.4	15.6	0.0%	0.0%
8	Savanna	52.3	5.5	0.0%	0.0%
9	Grassland	34.7	3.6	29.0%	81.8%
10	Crop land	190.0	19.8	100.0%	14.0%
	Total Area	958.6	100.0		

Overall Classification accuracy - 46.22%

Overall Kappa statistics - 0.34

3.8 Model Sensitivity

Tscalar was the most sensitive parameter followed by IPAR and FPAR in the model (Fig: 9). The least sensitive parameters were Wscalar and Pscalar. A variation of ±10% Tscalar can cause ±8% change in GPP estimates, while the same percentage variation in IPAR and FPAR can cause only ±4% change in GPP. The variation in Wscalar and Pscalar was negligible.

Table: 10. The changes in the cumulative composite of GPP (g C/m^2/8 days) in different vegetation types and different seasons according to i). present study, ii). MOD 17 A2 algorithm implemented using ground data and iii). MOD 17A2 GPP product using global datasets.

		EVR	Shola	DEC	Scrub	Grass	Tea	Teak
Yearly Avg.	Present study	12.8	6.4	11.9	10.6	1.4	3.1	11.7
	MOD 17A2 In-situ data	11.6	7.2	8.5	6.8	4.5	6.8	9.1
	MOD 17A2 GPP product	42.8	26.6	21.9	19.0	18.5	40.9	27.7
Dry Season Avg.	Present study	16.9	7.0	10.9	7.1	1.7	5.0	10.1
	MOD 17A2 In-situ data	18.1	9.9	10.0	7.9	6.4	10.0	12.2
	MOD 17A2 GPP product	59.6	35.4	23.9	21.1	23.6	54.8	35.4
Wet Season Avg.	Present study	8.8	5.7	12.8	14.1	1.1	1.2	13.2
	MOD 17A2 In-situ data	5.1	4.6	7.0	5.6	2.7	3.6	5.8
	MOD 17A2 GPP product	25.9	17.8	19.8	17.1	13.5	26.9	20.0

Fig: 12. Sensitivity of GPP to its input variables in Anamalai hills of Western Ghats, India. Out of five parameters (Tscalar, Wscalar, Pscalar, IPAR and FPAR), Tscalar is the most sensitive parameter in the model.

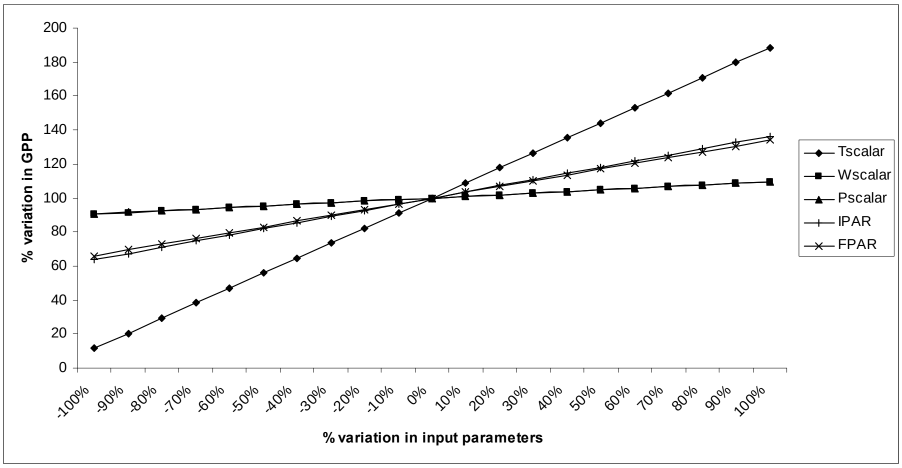

4. Discussion

4.1. Model inputs, framework and environmental settings

4.1.1. Data Availability

The study was undertaken with the aim to identify the challenges in the operational monitoring of carbon flux in tropical forests of India. Therefore, the first thing to mention is that the availability of the data. Though the daily images from MODIS Terra sensor were available, the cloud problem was a limiting factor for the use of data on a daily basis. The problem was most prominent in the monsoon (wet) period. It was very difficult to find a data which is cloud free in monsoon season. At the same time, 100% clouds were observed in few days. Those images were not considered in the analysis. Therefore, on an average, 5-6 days images were missing per month.

4.1.2. Model formulation

Two things are very important in any modelling studies; the first one is the model logic (how the model is logically organized) and the second one is the accuracy or resolution of the input data. In the present study, the model is organized in a logical manner by taking into consideration of the local environmental conditions. Temperature is a limiting factor or constraint in the photosynthetic process in higher elevation areas in the study area. Water is a stress factor in rainshadow regions or eastern side of the Western Ghats. Since 50% of the area belong to deciduous phenology, it was necessary to include a phenological measurement in the model. The area includes sparse vegetation (thorn forest) to dense vegetation (evergreen) and therefore, an index is required which is insensitive to background soil reflectance and high biomass condition. By considering all these parameters, the model logic suggested by Xiao et al. (2004) in Vegetation Production Model is found most appropriate to the study area.

In terms of resolution of data, a data was required which could be utilized for the operational monitoring carbon flux. MODIS could be considered as a sensible sensor in the trade-off between spatial resolution and temporal resolution. Daily data at 500 m resolution is quite reasonable to get information about the properties of vegetative surfaces. The maximum light use efficiency, a vegetation specific property, needs to be mapped at a better resolution since the area is highly heterogeneous. At the same time, it was not easy to go at the species assemblages level due to the inadequacy of the physiological information of these species. Therefore, as an agreement, 24 m resolution IRS P6 LISS III data was selected which was sufficient enough to provide land cover types with an accuracy of 80%. Daily weather observations were another major inputs in the model. The spacing of four weather stations in and around the areas was sufficiently enough to provide the information according to the standard climate reference guides (Linacre 1992).

4.1.3. Seasonal influence

The influence of monsoon is very clear in the hills. There are two types of monsoon in the study area. The first one is the south west monsoon which starts in the month of June and retrieve by first half of August and the second one, called north-east monsoon, starts in the second half of August and extend up to November. Due to this time lag, the month of August experience relatively low amount of rainfall compared to the preceding and following months as is evident from the figure: 4. In addition, the amount of rainfall received in the western part of the sanctuary was higher than eastern part. The western side of the sanctuary is windward side of Western Ghats and therefore, the quantity of precipitation (mainly orographic rainfall) is higher at west whereas precipitation is lower at east due to its leeward position. The western part of the sanctuary is approximately 75 km away from the coast and the monsoon current which flows through humid area condensed and precipitated by hitting on the mountain ranges (orographic rainfall). In the case of north-east monsoon, the current coming through the dry parts of Peninsular India by travelling hundreds of kilometres and the intensity reduced significantly before hitting the mountain ranges and therefore the amount of rainfall is much lower than the amount receives in the west.

4.1.4. Vegetation Types

The distribution of vegetation was according to the prevailing environmental conditions in the area. The western part of the study area where high amount of rainfall available is characterised by luxurious rainforest whereas the drier parts in east is characterised by deciduous forest. In addition to this common trend, the local distribution of vegetation communities was a function of topography of the area. The slopes in the mountainous areas (>1500m) support typical wet temperate forest (shola forest), whereas tops of the mountains are characterized by extensive stretches of grasslands. The upper elevation areas (> 800m) are characterised by evergreen forest, medium elevation areas by deciduous forest and low elevation areas by thorn-scrub forest. The occurrence of plantations in the area dates back to end of 18th century. About 150 years ago, these hills contained undisturbed and contiguous tracts of forest, but they were opened for plantations during the last century (Congreve 1938; Sundararaju 1987). The medium elevation and medium rainfall areas in the Top slip plateau were used for teak plantations and higher elevation and rainfall areas in the Valparai Plateau were used for tea plantations. This history is reflected in the extensive distributions of plantations now observed in the vegetation type map. In addition, there are about 36 tribal settlements inside the sanctuary and agriculture is the most common occupation for these villagers .

4.2. Model results

4.2.1. Maximum LUE

In light use efficiency models, maximum light use efficiency (ε_0) is considered as a constant for individual biomes. But in reality, biome is a very large spatial unit which could be considered as an aggregation of dynamic small spatial units. Interannual dynamics, land use changes, disturbance history, and different successional stages of vegetation may result in the spatial variation and temporal changes of ε_0 within a biome type. So it is possible that ε_0 at the canopy level is site-specific. The study area contains as much as fourteen natural vegetation communities or species assemblages in addition to the non-forest classes. Moreover, a number of disturbance factors are prevalent in the study area which maintains secondary forest formations (Joseph et al. in press). Any of these factors were not considered while assigning a constant value to the specific biome type. The major reason was the unavailability of the information. The maximum possible information about the ε_0 was available from Biome-BGC model and therefore, those values were assigned for biome types.

4.2.2. Selection of Indices

A number of studies have shown that changes in water content in plant tissues have a large effect on the leaf reflectance in the SWIR band region of the spectrum. It is well known that a large absorption by leaf water occurs in this region and therefore shortwave infrared reflectance (SWIR) reflectance is negatively related to leaf water content (Tucker 1980, Bowman, 1989, Ceccato et al. 2001). MODIS has two discrete channels in the SWIR (channel 5 is from 1230 to 1250 nm and channel 6 is from 1628 to 1652 nm) with a signal to noise ratio above 100 (Guenther et al. 2002). Studies by Fensholt and Sandholt (2003) and Fensholt et al (2006) indicated that water stress index based on channel 6 is performing better than channel 5 in Sahelian environment. They have recorded a correlation of 0.87 and 0.79 for channel 6 and channel 5 respectively. The present study also recorded a similar observation that water stress index based on channel 6 is performing better than channel 5. The R^2 values were 0.71 and 0.64 respectively. Xiao et al (2004a) have also used the water stress index based on channel 6 (LSWI) in their vegetation production model.

Comparison of vegetation indices with biomass values indicates that EVI is performing slightly better than NDVI. The advantage of using EVI lies in two properties. The first one is that it is not saturating at high biomass conditions. The second one is that it is less sensitive to atmospheric conditions and soil background reflectance (Huete et al. 2002). In the present study, both vegetation indices were not found saturated. Therefore, linear curves were fit into the data to know the R^2 value and to compare the relative performance. The second advantage was not tested due to the unavailability of ground data. The better performance of EVI in GPP modelling was noted recently and attempts were made to predict GPP solely based on EVI. Xiao et al (2004a, b) found a strong positive correlation between photosynthetically active vegetation and EVI, both for evergreen and deciduous forests. Rahman et al. (2005) noted a strong overall relationship between the MODIS 16 day EVI product and GPP across ten AmeriFlux tower sites representing a wide range of vegetation types. Sims et al. (2006) demonstrated that EVI alone could provide estimates of GPP that were as good as or better than MOD17 for nine flux tower site in North America during the active photosynthesis period. Sims et al. (2008) further explored to predict GPP based on EVI and LST (Land Surface Temperature) in their Temperature-Greenness (TG) model which excludes biome level look up table and coarse scale meteorological data.

4.2.3. Gross Primary Productivity

The maximum carbon assimilation is observed in those areas where there are no physical constraints. Phenologically, these areas are dominated by evergreen forests within an altitudinal range of 800 – 900 m. The lower value of GPP in deciduous forest in dry season was probably due to the water and phenological stresses. In wet season, the deciduous-scrub system showed higher assimilation rate due to the absence of limiting factors in physiological processes. The lowest values are observed in mountain grasslands and shola forest systems where temperature is the most important constraint.

4.3. Model comparison

The MODIS land cover product showed extremely low accuracy in the study area. The major vegetation type in the area, i.e., broadleaved deciduous forest was nearly absent and most of this vegetation type is mapped as crop land in the land cover product. The estimated accuracy was 42% which was much lower than the estimates available in literature. Hansen et al (2000) and Heinsch et al (2003) reported the accuracy of the product within a range of 65-80%. The misclassification between savanna and grassland may not have a significant implication in the GPP estimates since both the biome types have more or less similar ε_0. But the mapping of deciduous forest as cropland has much more implications since the ε_0 of cropland is almost half of deciduous forest.

The change in GPP estimate due to the difference in the resolution of input datasets was very prominent compared to the difference in algorithms. When local datasets having high resolution are used in both the models, the difference in the GPP estimate was negligible. When the same algorithm is implemented using global datasets, the GPP estimate was almost three times higher than the GPP estimate by local datasets. The resolution of this global DAO meteorological datasets is 1^0 which correspond approximately 100 km in the study area. A wide range of weather conditions exists in this interval as it clear from observations from local weather stations. The amount of IPAR varied almost double especially in wet season from station 1 to station 4. A similar trend was observed in case of temperature and relative humidity. Altitudinal variation may have a significant influence in micrometeorological conditions. The elevation in study area varies from 250 to 2500 m from eastern plains to high ranges in the west. The observed temperature lapse rate in the western side of the hills is 5.5^0C/km while it is 7.6^0C/km in the eastern side of the hills (Linacre 1992). Such large fluctuation might not be counted in the global datasets.

4.4. Model sensitivity

The most sensitive parameter in the model was temperature scalar. This was primarily due to the variability in the temperature throughout the landscape. The mountain tops recorded a temperature of 0^0C in winter season whereas the eastern plains recorded a temperature of 40^0C. The altitudinal difference, undulating terrain, and temperature lapse rate may be some of the parameters to be responsible for high sensitivity of Tscalar. Though a number of publications suggested an optimum temperature of 28^0C for tropical environment, there was confusion in assigning this value at the initial stage due to the diversity in the vegetation type. For example, the mountain tops experienced a temperate climatic system and the vegetation type in this area is considered as wet temperate forest according to the standard classification of Indian forest (Champion and Seth 1968). Therefore, a separate sensitivity analysis was conducted for a range of optimum temperature values from 20 to 28^0C. The analysis was conducted in uniform as well as stratified manners. Here, the uniform manner means a constant optimum temperature is assigned for all the vegetation types (for example 28^0C for deciduous and wet temperate forest) and stratified manner means different optimum temperatures were assigned to different vegetation types (for example, 28^0C for deciduous and 20^0C for wet temperate forest). The result showed that the variances are more or less similar in all the optimum temperature values and it was primarily due to topography of the landscape. The second most sensitive parameter was IPAR. This may be due to the prevalent and dynamic cloud conditions existing in the area. vanLaake and Sanchez-Azofeifa (2004 and 2005) reported that cloud optical thickness is the most sensitive parameter in tropical conditions and can hold back up to 50% of IPAR to reach the earth surface.

4.5. The question of validation

Though validation was not possible for the whole model due to the absence of ground measurements like eddy covariance towers, a stepwise validation procedure was followed in the course of study. The testing of relation between soil moisture and water stress indices, and biomass values and vegetation indices could be considered on that perspective. The other input variables (temperature, IPAR and relative humidity) in the model were locally available. Moreover, the study could be considered as a model study where fluxnet towers is limited (applicable to most of the old world tropics).

5. Conclusion

There is a trend among ecosystem modellers to work in those areas where enough databases are available. The limited studies in old world tropics, though it contributes ≈50% of total tropical forest area, could be attributed to this trend. In particular, there are no flux towers in South Asian forest including Indian forest. Therefore, none of the carbon assimilation models are calibrated and validated in this area. But efforts has been started to include these areas into the global network of ecosystem flux studies. At this context, the present study was undertaken to forecast the trend first by comparing the existing well known algorithms in operational monitoring, and thereafter check the efficacy of the models when the ground measurements are available. By taking this reverse approach, the bias of the analyst to fit the model to ground measured data could be eliminated.

The area selected for the study is the Anamalai hills in the Western Ghats biodiversity hotspot where the ecological setting is a representation of the diverse climatic and topographic gradients existing in peninsular India. The general objective was to assess the carbon assimilation of different vegetation types in different seasons. The following research questions are answered while achieving the objective.

Research Question: 1. Is advanced vegetation index such as EVI performing better than conventional vegetation index such as NDVI in tropical forest?

Method: The relative performance of vegetation indices was assessed by plotting the values of vegetation indices against sample plot biomass.

Result: A good positive relation was found between vegetation indices and biomass in evergreen and deciduous vegetation types. Enhanced Vegetation Index performed slightly better Normalized Differential Vegetation Index in both the vegetation types. The coefficient of determination (R^2) between EVI and biomass was 0.47 for evergreen forest and 0.39 for deciduous forest. For NDVI, the values were 0.38 and 0.34 respectively.

Conclusion: EVI is performing better than NDVI in tropical forest.

Research Question: 2. Which MODIS water stress index can better represent ground soil moisture condition?

Method: Correlation analysis was conducted between ground soil moisture data and MODIS water stress indices.

Result: Water stress index based on Channel 6 (Land Surface Water Index) yielded a correlation coefficient of 0.71 while Channel 5 (Shortwave Infrared Water Stress Index) yielded a value of 0.64.

Conclusion: Water stress index based on Channel 6 is performing better than the Channel 5.

Research Question: 3. How heterogeneity and seasonal changes in the vegetation types affect the carbon assimilation rate?

Method: A model is formulated to cover local environmental and vegetation-type specific factors. The variables included are the maximum light use efficiency of vegetation types (ε_0), controlling factors of ε_0, i.e., temperature, water and phenology, incoming PAR and fractional PAR that canopy absorbs. Carbon assimilation rate is estimated with respect to vegetation types and season-wise.

Result: The highest rate of carbon assimilation is observed in tropical wet evergreen forest especially lower elevation forest. The lowest rate of carbon assimilation is observed in grasslands. Tropical deciduous and thorn scrub forests showed a higher assimilation rate in wet season in comparison with dry season.

Conclusion: The area where there are limited physical constrains assimilate carbon at higher rate.

Research Question: 4. What are the sensitive parameters in the GPP model. How it affects the total estimates of GPP.

Method: The standard deviation of each input variable were altered by ±10% repeatedly while keeping the other variables constant and the corresponding change in GPP was noted.

Result: Temperature scalar was the most sensitive parameter followed by IPAR. A variation of ±10% Tscalar can cause ±8% change in GPP estimates, while the same percentage variation in IPAR can cause only ±4% change in GPP. This was primarily due to the topographic variability in the landscape and extreme cloud conditions respectively.

Conclusion: GPP estimation in heterogeneous mountain areas needs high resolution temperature and IPAR datasets.

Research Question: 5. How global level data products behave at local scale? Is there any variation in MOD 17 A2 GPP product when it is estimated at local scale? If yes, is it due to the algorithm difference or due to the changes in the resolution of the input datasets?

Method: The accuracy of the MODIS land cover product was tested using the ground control points. The variables in the MOD 17 A2, i.e., max LUE (ε_0), temperature minimum (TMIN) and vapour pressure deficit (VPD), IPAR and FPAR were calculated using local datasets and compared with globally derived estimates.

Result: MODIS land cover product showed an accuracy of 46%. Algorithm difference was not prominent in GPP estimate except for deciduous vegetation types. At the same time, estimates using global datasets were almost three times higher than the locally derived outputs.

Conclusion: Resolution of the input datasets plays a major role in GPP estimates rather than algorithm.

6. Reference

Baker, T.R., Oliver, L.P., Yadvinder, M., Samuel, A., Luzmila, A., Anthony Di, F., Terry, E., Niro, H., Timothy, J.K., Susan, G.L., William, F.L., Simon, L.L., Abel, M., David, A.N., Percy, N.V., Nigel, C.A.P., Natalino, M.S., and Rodolfo, V.M. 2004. Increasing Biomass in Amazonian Forest Plots. *Philosophical Transactions: Biological Sciences* **359**(1443): 353-365.

Blasco, F. 1970. Aspects of flora and ecology of the savannas of the south Indian hills. *Journal of the Bombay Natural History Society* **67**: 522-534.

Bowman, W.D. 1989. The relationship between leaf water status, gas exchange, and spectral reflectance in cotton leaves. *Remote Sensing of Environment* **30**(3): 249-255.

Brovkin, V., Levis, S., Loutre, M.-F., Crucifix, M., Claussen, M., Ganopolski, A., Kubatzki, C., and Petoukhov, V. 2003. Stability Analysis of the Climate-Vegetation System in the Northern High Latitudes. *Climatic Change* **57**(1): 119-138.

Ceccato, P., Flasse, S., Tarantola, S., Jacquemoud, S., and Grégoire, J.-M. 2001. Detecting vegetation leaf water content using reflectance in the optical domain. *Remote Sensing of Environment* **77**(1): 22-33.

Champion, H.G. and Seth, S.K. 1968. *A revised survey of the forest types of India.* Manager of Publications, Govt.of India, Delhi.

Chave, J., Andalo, C., Brown, S., Cairns, M.A., Chambers, J.Q., Eamus, D., Faister, H., Fromard, F., Higuchi, N., Kira, T., Lescure, J.P., Nelson, B.W., Ogawa, H., Puig, H., Riacra, B., and Yamakura, T. 2005. Tree allometry and improved estimation of carbon stocks and balance in tropical forests. *Oecologia* **145**(1): 87-99.

Chhabra, A. and Dadhwal, V.K. 2004. Assessment of major pools and fluxes of carbon in Indian forests. *Climatic Change* **64**: 341–360.

Congreve, C.R.T. 1938. *The Anamalais.* Tamil Nadu Forest Department, Madras.

Cramer, W., Kicklighter, D.W., Bondeau, A., Iii, B.M., Churkina, G., Nemry, B., Ruimy, A., Schloss, A.L., and Th, E.P.O.F.T.P.N.M.I. 1999. Comparing global models of terrestrial net primary productivity (NPP): overview and key results. *Global Change Biology* **5**(S1): 1-15.

Dadhwal, V.K. and Nayak, S.R. 1993. A Preliminary Estimate of Biogeochemical Cycle of Carbon for India. *Science and Culture* **59**: 9-13.

Dadhwal, V.K. and Shah, A.K. 1997. Recent Changes (1982-1991) in Forest Phytomass Carbon Pool in India Estimated Using Growing Stock and

Remote Sensing-Based Forest Inventories. *J Tropical Forestry* **13**: 182-188.

Dickinson, R.E. and Henderson-Sellers, A. 1988. Modelling tropical deforestation: A study of GCM land-surface parametrizations. *Quarterly Journal of the Royal Meteorological Society* **114**(480): 439-462.

Dixon, R.K., Solomon, A.M., Brown, S., Houghton, R.A., Trexier, M.C., and Wisniewski, J. 1994. Carbon Pools and Flux of Global Forest Ecosystems. *Science* **263**(5144): 185-190.

ERDAS. 2006. *ERDAS Iamgine tour guides*. Leica Geosystems Geospatial Imaging, LLC.

Fensholt, R. and Sandholt, I. 2003. Derivation of a shortwave infrared water stress index from MODIS near- and shortwave infrared data in a semiarid environment. *Remote Sensing of Environment* **87**(1): 111-121.

Fensholt, R., Sandholt, I., Rasmussen, M.S., Stisen, S., and Diouf, A. 2006. Evaluation of satellite based primary production modelling in the semi-arid Sahel. *Remote Sensing of Environment* **105**(3): 173-188.

Field, C.B., Randerson, J.T., and Malmstrom, C.M. 1995. Global Net Primary Production: Combining Ecology and Remote Sensing. *Remote Sensing of Environment* **51**(1): 74-88.

FSI. 2003. *State of Forest Report 2003*. Forest Survey of India, Government of India, Dehradun, India.

Gibbs, H.K., Brown S, Niles, J.O., and Foley, J.A. 2007. Monitoring and estimating tropical forest carbon stocks: making REDD a reality. *Environ Res Lett* **2**: 045023.

Glenn, E., Huete, A., Nagler, P., and Nelson, S. 2008. Relationship Between Remotely-sensed Vegetation Indices, Canopy Attributes and Plant Physiological Processes: What Vegetation Indices Can and Cannot Tell Us About the Landscape. *Sensors* **8**(4): 2136-2160.

Goetz, S.J., Prince, S.D., Goward, S.N., Thawley, M.M., Small, J., and Johnston, A. 1999. Mapping net primary production and related biophysical variables with remote sensing: Application to the BOREAS region. *J Geophys Res* **104**(D22): 27719-27734.

Goulden, M.L., Miller, S.D., da Rocha, H.R., Menton, M.C., de Freitas, H.C., e Silva Figueira, A.M., and de Sousa, C.A.D. 2004. Diel and seasonal patterns of tropical forest CO_2 exchange. *Ecological Applications* **14**(sp4): 42-54.

Guenther, B., Xiong, X., Salomonson, V.V., Barnes, W.L., and Young, J. 2002. On-orbit performance of the Earth Observing System Moderate Resolution

Imaging Spectroradiometer; first year of data. *Remote Sensing of Environment* **83**(1-2): 16-30.

Hansen, M.C. and Reed, B. 2000. A comparison of the IGBP DISCover and University of Maryland 1 km global land cover products. *International Journal of Remote Sensing* **21**(6): 1365-1373.

Heinsch F.A., Reeves M., Votava P., Kang S., Milesi C., Zhao M., Glassy J, Jolly WM, Loehman R, Bowker CF, Kimball JS, Nemani RS, and SW., R. 2003. User's Guide GPP and NPP (MOD17A2/A3) Products NASA MODIS Land Algorithm. NTSG, University of Montana, Montana.

Heinsch, F.A., Zhao, M., Running, S.W., Kimball, J.S., Nemani, R.R., Davis, K.J., Bolstad, P.V., Cook, B.D., Desai, A.R., Ricciuto, D.M., Law, B.E., Oechel, W.C., Kwon, H., Luo, H., Wofsy, S.C., Dunn, A.L., Munger, J.W., Baldocchi, D.D., Xu, L., Hollinger, D.Y., Richardson, A.D., Stoy, P.C., Siqueira, M.B.S., Monson, R.K., Burns, S.P., and Flanagan, L.B. 2006. Evaluation of Remote Sensing Based Terrestrial Productivity From MODIS Using Regional Tower Eddy Flux Network Observations. *IEEE Transactions on Geoscience and Remote Sensing* **44**(7-part-1): 1908-1925.

Hijmans, R.J., Cameron, S.E., Parra, J.L., Jones, P., and Jarvis, A. 2005. Very high resolution interpolated climate surfaces for global land areas. *International Journal of Climatology* **25**: 1965-1978.

Hilker, T., Coops, N.C., Wulder, M.A., Black, T.A., and Guy, R.D. 2008. The use of remote sensing in light use efficiency based models of gross primary production: A review of current status and future requirements. *Science of The Total Environment* **404**(2-3): 411-423.

Huete, A., Didan, K., Miura, T., Rodriguez, E.P., Gao, X., and Ferreira, L.G. 2002. Overview of the radiometric and biophysical performance of the MODIS vegetation indices. *Remote Sensing of Environment* **83**(1-2): 195-213.

Huete, A.R., HuiQing, L., and van Leeuwen, W.J.D. 1997. The use of vegetation indices in forested regions: issues of linearity and saturation. *Geoscience and Remote Sensing, 1997 IGARSS '97 'Remote Sensing - A Scientific Vision for Sustainable Development', 1997 IEEE International* **4**: 1966-1968 vol.1964.

IPCC. 2007. *Fourth Assessment Report of the Intergovernmental Panel on Climate Change - The Physical Science Basis*. Cambridge University Press, Cambridge, United Kingdom.

Ishida, A., Toma, T., and Marjenah. 1999. Limitation of leaf carbon gain by stomatal and photochemical processes in the top canopy of Macaranga conifera, a tropical pioneer tree. **19**: 467-473.

Ishigami, Y., Shimizu, Y., and Omasa, K. 2005. Evaluation of the risk to natural vegetation from climate change in Japan. *Journal of Agricultural Meteorology* **61**: 69-75.

Janzen, H.H. 2004. Carbon cycling in earth systems--a soil science perspective. *Agriculture, Ecosystems & Environment* **104**(3): 399-417.

Joseph, S., Reddy, C.S., Srivastava, V.K., Sudhakar, S., and Murthy, M.S.R. 2008. Mapping of national parks and wildlife sanctuaries-A pilot project: Indira Gandhi wildlife sanctuary. Report submitted to Ministry of Environment and Forests, Government of India.

Joseph, S., Blackburn, G.A., Gharai, B., Sudhakar, S., Thomas, A.P., and Murthy, M.S.R. in press. Monitoring conservation effectiveness in a global biodiversity hotspot: the contribution of land cover change assessment. *Environmental Monitoring and Assessment*, DOI 10.1007/s10661-008-0571-4.

Keeling, C. 1960. The concentration and isotopic abundance of carbon dioxide in the atmosphere. *Tellus B* **12**: 200-203.

Körner, C. 2004. Through enhanced tree dynamics carbon dioxide enrichment may cause tropical forests to lose carbon. *Philosophical Transactions of the Royal Society B: Biological Sciences* **359**(1443): 493-498.

Kyriakidis, P.C. and Dungan, J.L. 2001. A geostatistical approach for mapping thematic classification accuracy and evaluating the impact of inaccurate spatial data on ecological model predictions. *Environmental and Ecological Statistics* **8**(4): 311-330.

Lagergren, F., Eklundh, L., Grelle, A., Lundblad, M., Molder, M., Lankreijer, H., and Lindroth, A. 2005. Net primary production and light use efficiency in a mixed coniferous forest in Sweden. *Plant, Cell & Environment* **28**(3): 412-423.

Li, Z., Yu, G., Xiao, X., Li, Y., Zhao, X., Ren, C., Zhang, L., and Fu, Y. 2007. Modeling gross primary production of alpine ecosystems in the Tibetan Plateau using MODIS images and climate data. *Remote Sensing of Environment* **107**(3): 510-519.

Liang, S., T. Zheng, R. Liu, H. Fang, S.-C. Tsay, and Running, S. 2006. Estimation of incident photosynthetically active radiation from Moderate Resolution Imaging Spectrometer data. *J Geophys Res,* **111**: D15208.

Linacre, E. 1992. *Climate data and resources - A reference and guide*. Routledge, London and New York.

Liu, R., Shunlin, L., Honglin, H., Jiyuan, L., and Tao, Z. 2008. Mapping incident photosynthetically active radiation from MODIS data over China. *Remote Sensing of Environment* **112**(3): 998-1009.

Lobell, D.B., Asner, G.P., Law, B.E., and Treuhaft, R.N. 2002. View angle effects on canopy reflectance and spectral mixture analysis of coniferous forests using AVIRIS. *International Journal of Remote Sensing* **23**: 2247-2262.

Mahadevan, P., S. C. Wofsy, D. M. Matross, X. Xiao, A. L. Dunn, J. C. Lin, C. Gerbig, J. W. Munger, V. Y. Chow, and Gottlieb, E.W. 2008. A satellite-based biosphere parameterization for net ecosystem CO2 exchange: Vegetation Photosynthesis and Respiration Model (VPRM). *Global Biogeochem Cycles* **22**: GB2005.

Malcolm, J.R., Liu, C., Neilson, R.P., Hansen, L., and Hannah, L. 2006. Global warming and extinctions of endemic species from biodiversity hotspots. *Conservation Biology* **20**: 538-548.

Malhi, Y., Nobre, A.D., Grace, J., Kruijt, B., Pereira, M.G.P., Culf, A., and Scott, S. 1998. Carbon dioxide transfer over a Central Amazonian rain forest. *J Geophys Res* **103**: 31593 - 31612.

Malhi, Y. and Phillips, O.L. 2004. Tropical forests and global atmospheric change: a synthesis. *Philosophical Transactions of the Royal Society B: Biological Sciences* **359**(1443): 549-555.

Meroni, M. and Colombo, R. 2006. Leaf level detection of solar induced chlorophyll fluorescence by means of a subnanometer resolution spectroradiometer. *Remote Sensing of Environment* **103**(4): 438-448.

Monteith, J.L. 1972. Solar Radiation and Productivity in Tropical Ecosystems. *The Journal of Applied Ecology* **9**(3): 747-766.

Monteith, J.L. and Moss, C.J. 1977. Climate and the Efficiency of Crop Production in Britain [and Discussion]. *Philosophical Transactions of the Royal Society of London Series B, Biological Sciences* **281**(980): 277-294.

Moya, I., Camenen, L., Evain, S., Goulas, Y., Cerovic, Z.G., Latouche, G., Flexas, J., and Ounis, A. 2004. A new instrument for passive remote sensing - 1. Measurements of sunlight-induced chlorophyll fluorescence. *Remote Sensing of Environment* **91**(2): 186-197.

Murali, K.S., Bhat, D.M., and Ravindranath, N.H. 2005. Biomass estimation equations for tropical deciduous and evergreen forests. *Int J Agricultural Resources, Governance and Ecology* **4**(1): 81–92.

Myers, N., Mittermeier, R.A., Mittermeier, C.G., de Fonseca G.A.B. and Kent J. 2000. Biodiversity hotspots for conservation priorities. *Nature* **403**: 853-858.

Myneni, R.B., Hoffman, S., Knyazikhin, Y., Privette, J.L., Glassy, J., Tian, Y., Wang, Y., Song, X., Zhang, Y., Smith, G.R., Lotsch, A., Friedl, M., Morisette, J.T., Votava, P., Nemani, R.R., and Running, S.W. 2002. Global products of vegetation leaf area and fraction absorbed PAR from year one of MODIS data. *Remote Sensing of Environment* **83**(1-2): 214-231.

Nair, N.C. and Daniel, P. 1986. The floristic diversity of the Western Ghats and its conservation: a review. *Proceedings of the Indian Academy of Sciences (Animal Sciences/Plant Sciences Supplement)*: 127-163.

Nayar, M.P. 1996. *Hotspots of Endemic Plants of India*. Tropical Botanic Garden Research Institute, India.

Nemani, R.R., Keeling, C.D., Hashimoto, H., Jolly, W.M., Piper, S.C., Tucker, C.J., Myneni, R.B., and Running, S.W. 2003. Climate-Driven Increases in Global Terrestrial Net Primary Production from 1982 to 1999. *Science* **300**(5625): 1560-1563.

Olofsson, P., Eklundh, L., Lagergren, F., Jönsson, P., and Lindroth, A. 2007a. Estimating net primary production for Scandinavian forests using data from Terra/MODIS. *Advances in Space Research* **39**(1): 125-130.

Olofsson, P., Lagergren, F., A. Lindroth, J. Lindström, Klemedtsson, L., and Eklundh, L. 2007b. Towards operational remote sensing of forest carbon balance across Northern Europe. *Biogeosciences Discussions* **4**: 3143–3193.

Otterman, J., Chou, M.D., and Arking, A. 1984. Effects of Nontropical Forest Cover on Climate. *Journal of Applied Meteorology* **23**(5): 762-767.

Phillips, O.L., Baker, T.R., Arroyo, L., Higuchi, N., Killeen, T.J., Laurance, W.F., Lewis, S.L., Lloyd, J., Malhi, Y., Monteagudo, A., Neill, D.A., Núñez Vargas, P., Silva, J.N.M., Terborgh, J., Vásquez Martínez, R., Alexiades, M., Almeida, S., Brown, S., Chave, J., Comiskey, J.A., Czimczik, C.I., Di Fiore, A., Erwin, T., Kuebler, C., Laurance, S.G., Nascimento, H.E.M., Olivier, J., Palacios, W., Patiño, S., Pitman, N.C.A., Quesada, C.A., Saldias, M., Torres Lezama, A., and Vinceti, B. 2004. Pattern and process in Amazon tree turnover, 1976-2001. *Philosophical Transactions of the Royal Society B: Biological Sciences* **359**(1443): 381-407.

Phillips, O.L., Malhi, Y., Higuchi, N., Laurance, W.F., uacute, ntilde, ez, P.V., aacute, squez, R.M., Laurance, S.G., Ferreira, L.V., Stern, M., Brown, S., and Grace, J. 1998. Changes in the Carbon Balance of Tropical Forests: Evidence from Long-Term Plots. *Science* **282**(5388): 439-442.

Pons, T.L. and Welschen, R.A.M. 2003. Midday depression of net photosynthesis in the tropical rainforest tree Eperua grandiflora: contributions of stomatal and internal conductances, respiration and Rubisco functioning. Tree Physiology **23**: 937-947.

Potter, C., Randerson, J., Field CB, Matson PA, Vitousek PM, and Mooney HA. 1993. Terrestrial ecosystem production - a process model-based on global satellite and surface data. *Global Biogeochemical Cycles* **7**(4): 811-841.

Potter, C., Steven, K., and Vanessa, B. 1999. Interannual Variability in Terrestrial Net Primary Production: Exploration of Trends and Controls on Regional to Global Scales. *Ecosystems* **2**(1): 36-48.

Prince, S.D. and Goward, S.N. 1995. Global Primary Production: A Remote Sensing Approach. *Journal of Biogeography* **22**(4/5): 815-835.

Rahman, M.M., E. Csaplovics, and Koch, B. 2005. An efficient regression strategy for extracting forest biomass information from satellite sensor data. *International Journal of Remote Sensing* **26**: 1511-1519.

Raich, J.W., Rastetter, E.B., Melillo, J.M., Kicklighter, D.W., Steudler, P.A., Peterson, B.J., Grace, A.L., B. Moore, I., and Vorosmarty, C.J. 1991. Potential Net Primary Productivity in South America: Application of a Global Model. *Ecological Applications* **1**(4): 399-429.

Ramachandran, A., S. Jayakumar, R. M. Haroon, Bhaskaran, A., and Arockiasamy, D.I. 2007. Carbon sequestration: estimation of carbon stock in natural forests using geospatial technology in the Eastern Ghats of Tamil Nadu, India. *Current Science* **92**(3): 323-331.

Ravindranath, N.H., Somashekhar, B.S., and Gadgil, M. 1997. Carbon flow in Indian forests. *Climatic Change* **35**(3): 297-320.

Ruimy, A., P. G. Jarvis, D. D. Baldocchi, and Saugier, B. 1995. CO2 fluxes over plant canopies and solar radiation : A review. *Adv Ecol Res* **26**: 1 -68.

Running, S.W., Baldocchi, D.D., Turner, D.P., Gower, S.T., Bakwin, P.S., and Hibbard, K.A. 1999. A Global Terrestrial Monitoring Network Integrating Tower Fluxes, Flask Sampling, Ecosystem Modeling and EOS Satellite Data. *Remote Sensing of Environment* **70**(1): 108-127.

Running, S.W., Nemani, R.R., Heinsch, F.A., Zhao, M., Reeves, M., and Hashimoto, H. 2004. A Continuous Satellite-Derived Measure of Global Terrestrial Primary Production. *BioScience* **54**(6): 547-560.

Sims, D.A., Rahman, A.F., Cordova, V.D., El-Masri, B.Z., Baldocchi, D.D., Bolstad, P.V., Flanagan, L.B., Goldstein, A.H., Hollinger, D.Y., Misson, L., Monson, R.K., Oechel, W.C., Schmid, H.P., Wofsy, S.C., and Xu, L. 2008. A new model of gross primary productivity for North American ecosystems based solely on the enhanced vegetation index and land surface temperature from MODIS. *Remote Sensing of Environment* **112**(4): 1633-1646.

Sims, D.A., Rahman, A.F., Cordova, V.D., El-Masri, B.Z., Baldocchi, D.D., and Flanagan, L.B., et al. 2006. On the use of MODIS EVI to assess gross primary productivity of North American ecosystems. *Journal of Geophysical Research* **111**(G04015).

Sukumar, R., Suresh, H.S., and Ramesh, R. 1995. Climate change and its impact on tropical montane ecosystems in southern India. *Journal of Biogeography* **22**: 533-536.

Sundararaju, R. 1987. *Management Plan for Indira Gandhi Wildlife Sanctuary*. Office of the Chief Wildlife Warden, Chennai.

Sundareshwar, P.V., Murtugudde, R., Srinivasan, G., Singh, S., Ramesh, K.J., Ramesh, R., Verma, S.B., Agarwal, D., Baldocchi, D., Baru, C.K., Baruah, K.K., Chowdhury, G.R., Dadhwal, V.K., Dutt, C.B.S., Fuentes, J., Gupta, P.K., Hargrove, W.W., Howard, M., Jha, C.S., Lal, S., Michener, W.K., Mitra, A.P., Morris, J.T., Myneni, R.R., Naja, M., Nemani, R., Purvaja, R., Raha, S., Vanan, S.K.S., Sharma, M., Subramaniam, A., Sukumar, R., Twilley, R.R., and Zimmerman, P.R. 2007. ENVIRONMENT: Environmental Monitoring Network for India. *Science* **316**(5822): 204-205.

Thomas, C.D., Cameron, A., Green, R.E., Bakkenes, M., Beaumont, L.J., Collingham, Y.C., Erasmus, B.F.N., de Siqueira, M.F., Grainger, A., Hannah, L., Hughes, L., Huntley, B., van Jaarsveld, A.S., Midgley, G.F., Miles, L., Ortega-Huerta, M.A., Townsend Peterson, A., Phillips, O.L., and Williams, S.E. 2004. Extinction risk from climate change. *Nature* **427**(6970): 145-148.

Thornton, P.E., Law, B.E., Gholz, H.L., Clark, K.L., Falge, E., Ellsworth, D.S., Goldstein, A.H., Monson, R.K., Hollinger, D., Falk, M., Chen, J., and Sparks, J.P. 2002. Modeling and measuring the effects of disturbance history and climate on carbon and water budgets in evergreen needleleaf forests. *Agricultural and Forest Meteorology* **113**(1-4): 185-222.

Tian, H., Melillo, J.M., Kicklighter, D.W., McGuire, A.D., Helfrich, J.V.K., Moore, B., and Vorosmarty, C.J. 1998. Effect of interannual climate variability on carbon storage in Amazonian ecosystems. *Nature* **396**(6712): 664-667.

Tucker, C.J. 1980. Remote sensing of leaf water content in the near infrared. *Remote Sensing of Environment* **10**(1): 23-32.

Turner, D.P., Ritts, W.D., Cohen, W.B., Maeirsperger, T.K., Gower, S.T., Kirschbaum, A.A., Running, S.W., Zhao, M., Wofsy, S.C., Dunn, A.L., Law, B.E., Campbell, J.L., Oechel, W.C., Kwon, H.J., Meyers, T.P., Small, E.E., Kurc, S.A., and Gamon, J.A. 2005. Site-level evaluation of satellite-based global terrestrial gross primary production and net primary production monitoring. *Global Change Biology* **11**(4): 666-684.

Van Laake, P.E. and Sanchez-Azofeifa, G.A. 2004. Simplified atmospheric radiative transfer modelling for estimating incident PAR using MODIS atmosphere products. *Remote Sensing of Environment* **91**(1): 98-113.

Van Laake, P.E. and Sanchez-Azofeifa, G.A. 2005. Mapping PAR using MODIS atmosphere products. *Remote Sensing of Environment* **94**(4): 554-563.

White, M.A., Thornton, P.E., Running, S.W., and Nemani, R.R. 2000. Parameterization and Sensitivity Analysis of the BIOME–BGC Terrestrial Ecosystem Model: Net Primary Production Controls. *Earth Interactions* **4**(3): 1-85.

Xiao, X., Hollinger, D., Aber, J., Goltz, M., Davidson, E.A., Zhang, Q., and Moore, B. 2004a. Satellite-based modeling of gross primary production in an evergreen needleleaf forest. *Remote Sensing of Environment* **89**(4): 519-534.

Xiao, X., Zhang, Q., Braswell, B., Urbanski, S., Boles, S., Wofsy, S., Moore, B., and Ojima, D. 2004b. Modeling gross primary production of temperate deciduous broadleaf forest using satellite images and climate data. *Remote Sensing of Environment* **91**(2): 256-270.

Xiao, X., Zhang, Q., Saleska, S., Hutyra, L., De Camargo, P., Wofsy, S., Frolking, S., Boles, S., Keller, M., and Moore, B. 2005. Satellite-based modeling of gross primary production in a seasonally moist tropical evergreen forest. *Remote Sensing of Environment* **94**(1): 105-122.

Yuan, W., Liu, S., Zhou, G., Zhou, G., Tieszen, L.L., Baldocchi, D., Bernhofer, C., Gholz, H., Goldstein, A.H., Goulden, M.L., Hollinger, D.Y., Hu, Y., Law, B.E., Stoy, P.C., Vesala, T., and Wofsy, S.C. 2007. Deriving a light use efficiency model from eddy covariance flux data for predicting daily gross primary production across biomes. *Agricultural and Forest Meteorology* **143**(3-4): 189-207.

Zhao, M., Running, S.W., and Nemani, R.R. 2006. Sensitivity of Moderate Resolution Imaging Spectroradiometer (MODIS) terrestrial primary production to the accuracy of meteorological reanalyses. *J Geophys Res* **111**, DOI 10.1029/2004JG000004.